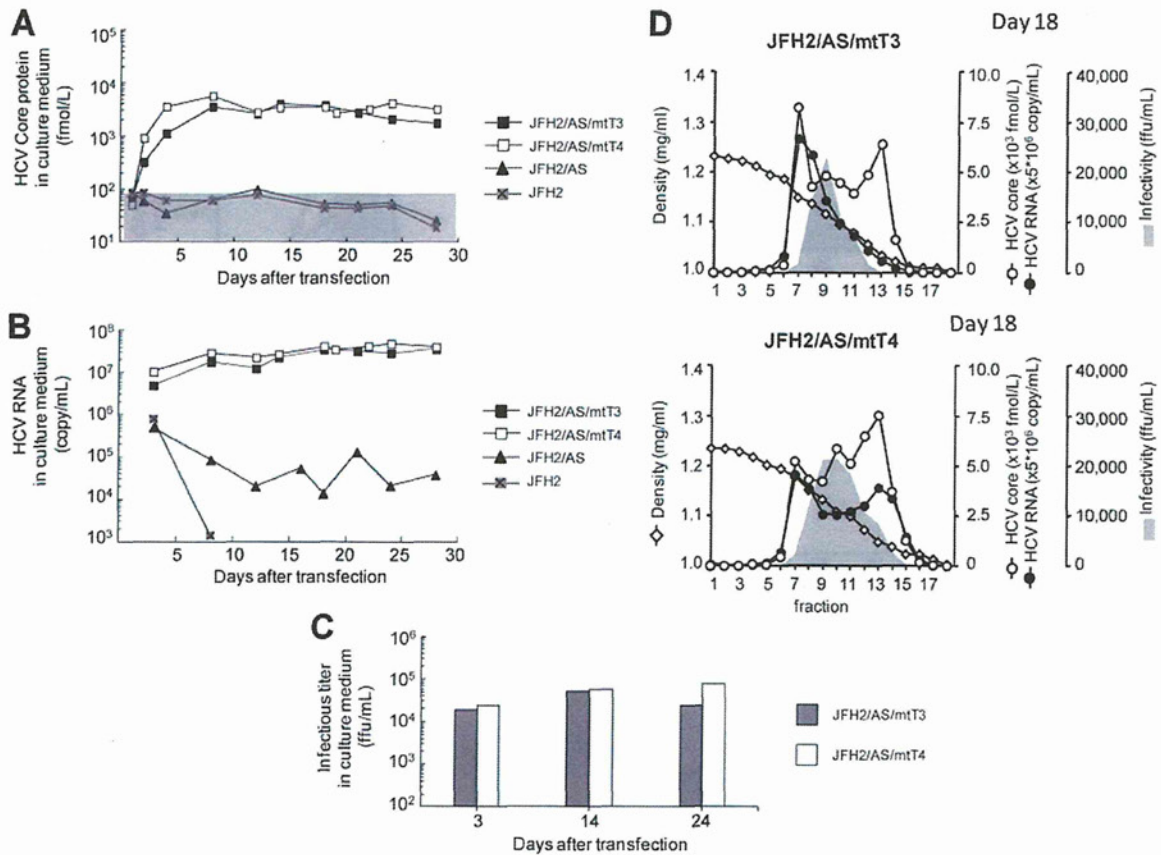FIG 10 Continuous passage of J6/JFH2/AS cell culture-adapted virus RNA-transfected cells. Full-length HCV RNA was synthesized from the J6/JFH2/AS, J6/JFH2/AS/mtT1A (mtT1A), and J6/JFH2/AS/mtT1B (mtT1B) constructs. RNA-transfected cells were serially passaged until 38 days after transfection, and culture supernatants were harvested at the indicated time points. HCV core protein (A) and HCV RNA (B) levels in the culture media were determined. The data in the gray area were below the detection limit of the assay to detect HCV core protein. (C) Infectivity in the culture medium was determined by focus formation assay at 5, 8, 14, 27, and 38 days after transfection.

also used for electron microscopy analysis. After the density gradient purification, spherical viral particles were detected (Fig. 7, right panel). After the core protein levels plateaued, naive Huh-7.5.1 cells were inoculated with the culture medium, as described above. When the core protein levels plateaued again after the third inoculation of T3 and T4 cells, we sequenced the viral genome in the culture medium (T3i3 and T4i3, respectively) to determine the adaptive mutation. We found the following nonsynonymous mutations: 414IT in E2, 1510EG and 1617RQ in NS3, 2006KQ, 2233AV and 2234NS in NS5A, and 2695TI in NS5B of T3i3; and 387VG in E1, 828VA in NS2, 1225RQ and 1283RG in NS3, 1883VA in NS4B, 2206SA, 2279KN, and 2441CR in NS5A, and 2695TI in NS5B of T4i3 (Fig. 3B). We introduced these mutations into the pJFH2/AS plasmid (pJFH2/AS/mtT3 and pJFH2/AS/mtT4). Synthesized RNA from pJFH2/AS/mtT3 and pJFH2/AS/mtT4 and the related control plasmids was transfected into Huh-7.5.1 cells. HCV core protein levels, HCV RNA levels, and infectivity were monitored in the culture medium of the transfected cells until 96 h after transfection (Fig. 9A to C). JFH2/AS/

mtT3 (mtT3) and JFH2/AS/mtT4 (mtT4) secreted similar levels of HCV core protein, RNA, and infectious virus with J6/JFH2/AS/mtT1A and J6/JFH2/AS/mtT1B. Although JFH2/AS/mtT3 secreted slightly higher levels of HCV core protein and RNA than JFH2/AS/mtT4, the secreted infectious virus titers were similar for both viruses. JFH2/AS/mtT3 and JFH2/AS/mtT4 RNA-transfected cells were also serially passaged, and the HCV core proteins were secreted immediately after transfection (Fig. 14A). However, JFH2 and JFH2/AS RNA-transfected cells did not secrete significant amounts of HCV core protein into the culture medium. HCV RNA levels in the culture medium of the RNA-transfected cells were at similar levels for JFH2/AS/mtT3 and JFH2/AS/mtT4 (around 10^7 copy/ml) (Fig. 14B). Infectivity was also detected as higher than 10^4 FFU/ml even at 3 days after the RNA transfection, and this level of infectious titer was maintained during the cell passages (Fig. 14C). We also analyzed JFH2/AS/mtT3 and JFH2/AS/mtT4 culture media by density gradient assay (Fig. 14D). The density profiles with HCV core protein and RNA levels and infectious titers in the fractions were basically similar to those of J6/JFH2/AS-adapted viruses (Fig. 6E and 11D). Taken together, the results described in this section indicate infectious virus was also recovered from the full-length JFH-2 construct with the 2217AS mutation.

Mechanistic analysis of adaptive mutations introduced in the J6/JFH2/AS and JFH2/AS cell culture-adapted viruses. To elucidate the mechanisms of adaptive mutations discovered in J6/JFH2/AS and JFH2/AS virus genomes, we transfected JFH-2 and J6/JFH2 constructs along with possible control constructs into Huh7-25 cells (2) (Fig. 15), which are CD81 defective. The transfection of JFH-1 RNA into Huh7-25 cells results in infectious HCV production, but there was no reinfection into Huh7-25 cells because the cell surface expression of CD81 is essential for HCV infection (10). HCV core protein levels were measured in the culture medium and cell lysate to monitor virus particle secretion and intracellular virus genome replication, respectively (Fig. 15A and B). JFH2/AS, JFH2, J6/JFH2, JFH1/GND, and J6/JFH2/GND RNA-transfected cells did not show increased levels of intracellular core protein expression. However, other RNA-transfected cells showed increased intracellular core protein expression. The cellular core protein level was especially increased at 72 and 96 h after transfection with J6/JFH2/AS RNA, which suggests a higher replication efficiency than J6/JFH; however, core protein secretion was not detected with J6/JFH2/AS, which suggests defective virus particle formation or secretion. Other adaptive mutations in J6/JFH2/AS/mtT1A and J6/JFH2/AS/mtT1B further increased virus genome replication and core protein secretion. In the case of JFH2/AS RNA transfection, cellular core protein expression was not detected, suggesting a lower replication efficiency than that of J6/JFH2/AS. This lower replication efficiency of JFH2/AS may be due to the presence of different sequences in the region of core protein to NS2. However, core protein expression in the cell lysate and culture medium was detected with both JFH2/AS/mtT3 and JFH2/AS/mtT4 RNA transfection. Thus, adaptive mutations in mtT3 and mtT4 are necessary to increase viral genome replication and efficient core protein secretion. JFH-1 and J6/JFH-1 had intracellular core protein expression levels that were similar and high. From the intracellular core protein data, it is clear that J6/JFH2/AS/mtT1A, J6/JFH2/AS/mtT1B, JFH2/AS/mtT3, and JFH2/AS/mtT4 constructs obtained higher replication capacities by

- 642 -

FIG 11 Serial passages of J6/JFH2/AS cell culture-adapted virus infected cells. Naive Huh-7.5.1 cells were inoculated with culture medium of the RNA-transfected cells at an MOI of 0.01. Inoculated cells were serially passaged, and culture supernatants were harvested at the indicated times. HCV core protein (A), HCV RNA (B), and infectivity (C) levels in the culture media were determined. (D) Density gradient analysis of culture supernatant from J6/JFH2/AS/mtT1A cell-culture adapted virus-infected Huh-7.5.1 cells. Culture supernatant of infected Huh-7.5.1 cells with mtT1A (day 8 [D8] D38 posttransfection) was harvested at 20 days after inoculation. Assays were performed as described in the legend of Fig. 6E. Open diamond, buoyant density.

FIG 12 Serum HCV RNA titer in human hepatocyte-transplanted uPA/SCID mice inoculated with JFH-2 serum and cell culture-adapted virus. Mice PXB 82-86 and PXB 82-90 were inoculated with the cell culture-adapted J6/JFH2/AS HCV particles, and mice PXB 83-2 and PXB 83-10 were inoculated with JFH-2 patient serum. Upper and lower panels indicate the results of the RT-PCR and the quantitative detection RT-PCR of HCV RNA in mouse serum, respectively.

adaptive mutations; however, their replication levels are lower than those of JFH-1 and J6/JFH1.

We also analyzed the ratio of extracellular protein to total core protein to analyze the virus secretion efficiency (Fig. 15C). J6/JFH-1 secreted a higher percentage of core protein into culture

FIG 13 Propagation of a full-length JFH2 virus. Huh-7.5.1 cells were transfected with the transcribed RNA from pJFH2/AS and pJ6/JFH2/AS. Two independently JFH2/AS RNA-transfected cell lines (T3 and T4) were independently passaged. At each time point, culture medium was harvested and analyzed for the presence of HCV core protein.

- 643 -

FIG 14 Full-length RNA was synthesized from the JFH2 construct and its derivatives with mutations. RNA-transfected cells were serially passaged, and culture supernatants were harvested at the indicated time points. HCV core protein (A), HCV RNA (B), and infectivity (C) levels in the culture media were determined. The data in the gray area were below the detection limit of the assay to detect HCV core protein. (D) Density gradient analysis of culture supernatant from JFH2/AS cell-culture adapted virus-infected Huh-7.5.1 cells. Culture supernatants of Huh-7.5.1 cells infected with JFH2/mtT3 and JFH2/mtT4 viruses were harvested 18 days after inoculation. Assays were performed as described in the legend of Fig. 6E. Open diamond, buoyant density.

medium than JFH-1. J6/JFH2/AS/mtT1A, J6/JFH2/AS/mtT1B, JFH2/AS/mtT3, and JFH2/AS/mtT4 RNA-transfected cells showed different percentages of secreted core protein. mtT1A and mtT1B constructs showed similar replication levels (Fig. 15B), but mtT1B showed a higher percentage of core protein secretion than mtT1A (Fig. 15C). mtT3 and mtT4 showed similar percentages of core protein secretion, which are higher than the level of JFH1 (Fig. 15C). Because J6/JFH2/AS RNA-transfected cells did not secrete core protein despite intracellular core protein expression (Fig. 15A and B), the adaptive mutant constructs obtained core protein (or virus particle) secretion phenotypes. Thus, during the adaptation process, the viruses obtained both higher replication capacity and core protein secretion capacity by their adaptive mutations.

Other HCV constructs with the 2217AS mutation. The alanine residue at amino acid position 2217 is located in the ISDR of NS5A, and it is conserved among HCV strains including genotype 1 and 2 strains. Because the 2217AS mutation in NS5A is the key mutation for the production of cell culture-adapted HCV, we introduced this mutation into other wild-type HCV constructs, i.e., H77 (genotype 1a), Con1 (genotype 1b), and J6CF (genotype 2a). Synthetic RNAs including the 2217AS mutation were electroporated into Huh-7.5.1 cells, and then the transfected cells were se-

rially passaged. HCV core protein secretion was measured in the culture medium of transfected cells. However, we could not observe the increment of HCV core levels in the culture medium (data not shown). Therefore, we concluded that the 2217AS mutation does not always induce cell culture adaptation in HCV isolates.

DISCUSSION

In previous studies, we have isolated cell culture-infectious HCV, the JFH-1 strain, from a patient with fulminant hepatitis (14, 38). In this report, we isolated another HCV cDNA, named JFH-2, also from a fulminant hepatitis patient. We constructed a subgenomic replicon with the JFH-2 sequence, but its replication efficiency was low. Among the mutations found in the replicon genome, the 2217AS mutation in the ISDR exhibited the strongest adaptive effect. Interestingly, the full-length chimeric or wild-type JFH-2 genome with adaptive mutations could replicate and produce infectious virus particles. Virus infection efficiency was sufficient for autonomous virus propagation in cultured cells.

Several full-length HCV cDNAs have been cloned, and their infectivity has been confirmed in vivo with chimpanzee models (18, 39). However, it has been difficult to produce recombinant viral particles and test their infectivity by using cell culture
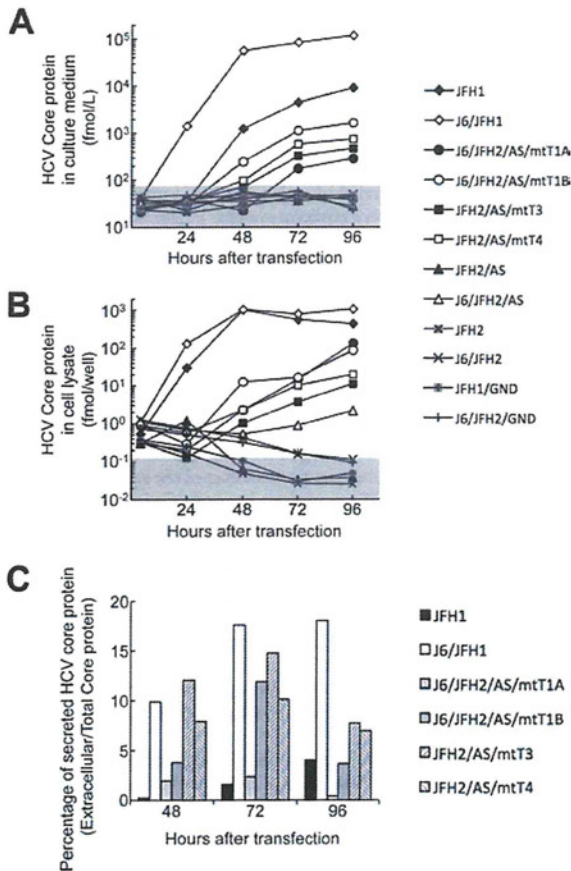
FIG 15 Transient virus production assay of J6/JFH2- and JFH2-related constructs with CD81-defective Huh7-25 cells. Full-length HCV RNA was synthesized from the JFH1, J6/JFH1, JFH2, and J6/JFH2 constructs and their derivatives with mutations and transfected into Huh7-25 cells. (A) HCV core protein levels in culture medium were determined at 4, 24, 48, 72, and 96 h after transfection. The data in the gray area were below detection limit. (B) HCV core protein levels in the cell lysate were determined at 24, 48, 72, and 96 h after transfection. (C) Percentages of secreted HCV core protein from the transfected cells were determined at 48, 72, and 96 h after transfection. Percentages of secreted HCV core protein were calculated only for the indicated viruses. All assays were performed in duplicate, and the data represent average values.

systems (4, 28). Only the JFH-1 strain efficiently replicates in HuH-7 cells and other hepatic and nonhepatic cell lines in subgenomic replicon form (20, 38, 41). Full-length wild-type JFH-1 RNA and chimeric JFH-1 RNA can replicate in HuH-7 cells and produce infectious virus. Since the JFH-1 strain was isolated from a patient with fulminant hepatitis, we assumed that virus strains that cause fulminant hepatitis may replicate efficiently in cultured cells. To identify more HCV clones that can replicate in cultured cells, we isolated the JFH-2 strain from another fulminant hepatitis patient (15). Interestingly, the JFH-2 strain showed a low level of replication in cultured cells in the initial subgenomic replicon experiment. This result may suggest that HCV strains isolated from fulminant hepatitis patients are able to replicate more efficiently than strains from chronic hepatitis patients; however, this hypothesis should be confirmed by testing more HCV strains from patients with fulminant hepatitis. The JFH-2 patient received a course of betamethasone therapy and developed fulminant hepatitis af-

ter the withdrawal of betamethasone. It is thus possible that the JFH-2 strain obtained its higher replication capacity in the immune-suppressed host environment. To confirm this hypothesis, we must test the replication efficiency of HCV strains isolated from other immune-suppressed patients, such as patients who are coinfected with HIV, patients who are reinfected after a transplant, and patients who are treated with immunosuppressive agents.

In previous reports, adaptive mutations have been found to enhance viral RNA replication at the expense of virus particle formation efficiency (28). A highly cell culture-adapted Con1 strain can replicate in cultured cells, but it cannot produce infectious virus particles. Interestingly, a highly adapted Con1 strain was not infectious for chimpanzees, while moderately adapted Con1 was infectious. However, the virus recovered from the infected animal was wild-type Con1 virus (5). This result clearly suggests that HCV strains with lower replication efficiencies are favorable for *in vivo* infection. However, we must note that the "replication efficiency" is determined in cultured cells. In the case of JFH-2, we found several adaptive mutations in the subgenomic replicon clones, and the most adaptive mutation, 2217AS, was tested in full-length HCV replication and virus production. After the RNA transfection of J6/JFH2/AS, we could not detect substantial virus secretion for about 30 days. However, after 30 days, significant levels of infectious virus particles were secreted into the culture medium. Naive Huh-7.5.1 cells were inoculated three times with the cell culture-adapted virus. This virus adaptation was also tested with full-length JFH2/AS, and we successfully obtained infectious JFH2/AS virus. Both the J6/JFH2/AS and JFH2/AS viruses acquired the ability for autonomous virus expansion in Huh-7.5.1 cells, and several additional mutations were found in their genomes. Interestingly, the 2695TI mutation in NS5B was commonly found in all of the adapted virus genomes, and isoleucine at amino acid position 2695 is also found in the JFH-1 strain. However, the introduction of only the 2695TI mutation into the J6/JFH2/AS or JFH2/AS virus genome did not restore robust virus production (data not shown). After repeated virus passages, mutations were found throughout the viral genome (in J6/JFH2/AS-T1Ai3 and -T1Bi3 and in JFH2/AS-T3i3 and -T4i3), and we are currently investigating which mutations or combinations of mutations are most important for this adaptation. From the comparisons of cell culture-adapted viruses and their parental virus constructs, adaptive mutations are necessary to increase both viral genome replication and virus particle assembly/secretion efficiency (Fig. 15). The procedure to produce cell culture-adapted HCV was thus established. The adaptive mutations found from the subgenomic replicon assay were introduced into the full-length genome, and the cells transfected with virus RNA were repeatedly passaged until the virus particles were produced.

In vivo infectivity may be inversely related to the replication efficiency in cultured cells, as discussed above. The original JFH-2 patient serum was infectious in human liver-transplanted mice; however, cell culture-adapted J6/JFH2/AS virus was not infectious. The JFH-1 virus was infectious not only for cultured cells but also for chimpanzees and human liver-transplanted mice (10, 38). However, the JFH-1 infection in chimpanzees was only mild and transient without any liver pathology. Thus, the J6/JFH2/AS and JFH2/AS viruses are more cell culture-adapted and attenuated than the JFH-1 virus. It may be worthwhile to test this cell culture-

- 645 -

adapted strain as a live attenuated vaccine candidate to induce protective immunity. However, for ethical reasons, the necessary chimpanzee experiments are not appropriate to perform. Therefore, we should wait for the establishment of immunocompetent small-animal models susceptible to HCV infection to perform this kind of study. Furthermore, future studies should examine the *in vivo* infectivity of the adapted J6/JFH2 and JFH2 viruses isolated in the present study.

The 2217AS mutation is located in the ISDR. In the previous study of the genotype 1b subgenomic replicon, mutations introduced into the ISDR enhanced the colony formation efficiency of the HCV replicons (17, 23). However, mutations in the ISDR impaired the genotype 1b HCV replication in human liver-transplanted mice (9). The exact mechanism of the ISDR is still not clear although the number of mutations in the ISDR is related to the efficacy of interferon therapy (8). Our results in this study also support the concept that the 2217AS mutation in the ISDR enhances replicon replication efficiency although the J6/JFH2/AS virus did not infect human liver-transplanted mice. Further studies are necessary to understand the molecular mechanism of the effects of adaptive mutations in the ISDR.

In the present study, we established a cell culture-adapted HCV strain, JFH-2. The virus could be passaged continuously in naive Huh-7.5.1 cells. This approach may be applicable to the establishment of new infectious HCV clones. Novel antiviral drugs are under development, and some of them will be used in the clinical setting. However, most of them target genotype 1 HCV strains. To eradicate other genotypes of HCV, it is important to establish their replicons and infectious virus culture systems.

ACKNOWLEDGMENTS

REFERENCES

1. Aizaki H, et al. 2008. Critical role of virion-associated cholesterol and sphingolipid in hepatitis C virus infection. J. Virol. 82:5715–5724.
2. Akazawa D, et al. 2007. CD81 expression is important for the permissiveness of Huh7 cell clones for heterogeneous hepatitis C virus infection. J. Virol. 81:5036–5045.
3. Akazawa D, et al. 2011. Production and characterization of HCV particles from serum-free culture. Vaccine 29:4821–4828.
4. Bartenschlager R, Lohmann V. 2000. Replication of hepatitis C virus. J. Gen. Virol. 81:1631–1648.
5. Bukh J, et al. 2002. Mutations that permit efficient replication of hepatitis C virus RNA in Huh-7 cells prevent productive replication in chimpanzees. Proc. Natl. Acad. Sci. U. S. A. 99:14416–14421.
6. Choo QL, et al. 1989. Isolation of a cDNA clone derived from a blood-borne non-A non-B viral hepatitis genome. Science 244:359–362.
7. Di Bisceglie AM, Hoofnagle JH. 2002. Optimal therapy of hepatitis C. Hepatology 36:S121–S127.
8. Enomoto N, et al. 1995. Sensitivity to interferon is conferred by amino acid substitutions in the NS5A region. J. Clin. Invest. 96:224–230.
9. Hiraga N, et al. 2011. Impact of viral amino acid substitutions and host interleukin-28b polymorphism on replication and susceptibility to interferon of hepatitis C virus. Hepatology 54:764–771.
10. Kato T, et al. 2008. Hepatitis C virus JFH-1 strain infection in chimpanzees is associated with low pathogenicity and emergence of an adaptive mutation. Hepatology 48:732–740.
11. Kato T, et al. 2003. Efficient replication of the genotype 2a hepatitis C virus subgenomic replicon. Gastroenterology 125:1808–1817.
12. Kato T, et al. 2005. Detection of anti-hepatitis C virus effects of interferon and ribavirin by a sensitive replicon system. J. Clin. Microbiol. 43:5679–5684.
13. Kato T, et al. 2006. Cell culture and infection system for hepatitis C virus. Nat. Protoc. 1:2334–2339.
14. Kato T, et al. 2001. Sequence analysis of hepatitis C virus isolated from a fulminant hepatitis patient. J. Med. Virol. 64:334–339.
15. Kato T, et al. 2003. Processing of hepatitis C virus core protein is regulated by its C-terminal sequence. J. Med. Virol. 69:357–366.
16. Kiyosawa K, et al. 1990. Interrelationship of blood transfusion, non-A, non-B hepatitis and hepatocellular carcinoma: analysis by detection of antibody to hepatitis C virus. Hepatology 12:671–675.
17. Kohashi T, et al. 2006. Site-specific mutation of the interferon sensitivity-determining region (ISDR) modulates hepatitis C virus replication. J. Viral Hepat. 13:582–590.
18. Kolykhalov AA, et al. 1997. Transmission of hepatitis C by intrahepatic inoculation with transcribed RNA. Science 277:570–574.
19. Kuo G, et al. 1989. An assay for circulating antibodies to a major etiologic virus of human non-A non-B hepatitis. Science 244:362–364.
20. Lindenbach BD, et al. 2005. Complete replication of hepatitis C virus in cell culture. Science 309:623–626.
21. Lindenbach BD, et al. 2006. Cell culture-grown hepatitis C virus is infectious in vivo and can be recultured in vitro. Proc. Natl. Acad. Sci. U. S. A. 103:3805–3809.
22. Lohmann V, et al. 1999. Replication of subgenomic hepatitis C virus RNAs in a hepatoma cell line. Science 285:110–113.
23. Maekawa S, et al. 2004. Introduction of NS5A mutations enables subgenomic HCV replicon derived from chimpanzee-infectious HC-J4 isolate to replicate efficiently in Huh-7 cells. J. Viral Hepat. 11:394–403.
24. McHutchison JG, et al. 1998. Interferon alfa-2b alone or in combination with ribavirin as initial treatment for chronic hepatitis C. N. Engl. J. Med. 339:1485–1492.
25. Merck & Co. 2011. Victrelis (boceprevir) prescribing information. Merck & Co., Whitehouse Station, NJ. http://www.accessdata.fda.gov/drugsatfda _docs/label/2011/202258lbl.pdf.
26. Murayama A, et al. 2007. The NS3 helicase and NS5B-to-3′X regions are important for efficient hepatitis C virus strain JFH-1 replication in Huh7 cells. J. Virol. 81:8030–8040.
27. Murayama A, et al. 2010. RNA polymerase activity and specific RNA structure are required for efficient HCV replication in cultured cells. PLoS Pathog. 6:e1000885. doi:10.1371/journal.ppat.1000885.
28. Pietschmann T, et al. 2002. Persistent and transient replication of full-length hepatitis C virus genomes in cell culture. J. Virol. 76:4008–4021.
29. Pietschmann T, et al. 2009. Production of infectious genotype 1b virus particles in cell culture and impairment by replication enhancing mutations. PLoS Pathog. 5:e1000475. doi:10.1371/journal.ppat.1000475.
30. Poynard T, et al. 1998. Randomised trial of interferon α2b plus ribavirin for 48 weeks or for 24 weeks versus interferon α2b plus placebo for 48 weeks for treatment of chronic infection with hepatitis C virus. Lancet 352:1426–1432.
31. Saeed M, et al. 2009. Evaluation of hepatitis C virus core antigen assays in detecting recombinant viral antigens of various genotypes. J. Clin. Microbiol. 47:4141–4143.
32. Takahashi H, et al. 2010. Biological properties of purified recombinant HCV particles with an epitope-tagged envelope. Biochem. Biophys. Res. Commun. 395:565–571.
33. Tateno C, et al. 2004. Near completely humanized liver in mice shows human-type metabolic responses to drugs. Am. J. Pathol. 165:901–912.
34. U. S. Food and Drug Administration. 2011. FDA news release. FDA approves Incivek for hepatitis C. U.S. Food and Drug Administration, Silver Spring, MD. http://www.fda.gov/NewsEvents/Newsroom/Press Announcements/ucm256299.htm.
35. U. S. Food and Drug Administration. 2011. FDA news release. FDA approves Victrelis for hepatitis C. U.S. Food and Drug Administration,

- 646 -

Silver Spring, MD. http://www.fda.gov/NewsEvents/Newsroom/Press Announcements/ucm255390.htm.

36. **Vertex Pharmaceuticals.** 2011. Incivek (telaprevir) prescribing information. Vertex Pharmaceuticals, Cambridge, MA. http://www.accessdata.fda .gov/drugsatfda_docs/label/2011/201917lbl.pdf.

37. **Wakita T.** 2009. Isolation of JFH-1 strain and development of an HCV infection system. Methods Mol. Biol. **510**:305–327.

38. **Wakita T, et al.** 2005. Production of infectious hepatitis C virus in tissue culture from a cloned viral genome. Nat. Med. **11**:791–796.

39. **Yanagi M, Purcell RH, Emerson SU, Bukh J.** 1997. Transcripts from a single full-length cDNA clone of hepatitis C virus are infectious when directly transfected into the liver of a chimpanzee. Proc. Natl. Acad. Sci. U. S. A. **94**:8738–8743.

40. **Yanagi M, Purcell RH, Emerson SU, Bukh J.** 1999. Hepatitis C virus: an infectious molecular clone of a second major genotype (2a) and lack of viability of intertypic 1a and 2a chimeras. Virology **262**:250–263.

41. **Zhong JP, et al.** 2005. Robust hepatitis C virus infection in vitro. Proc. Natl. Acad. Sci. U. S. A. **102**:9294–9299.

ELSEVIER
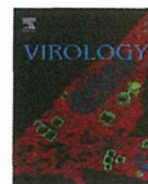
Trans-complemented hepatitis C virus particles as a versatile tool for study of virus assembly and infection

Ryosuke Suzuki [a,*], Kenji Saito [a], Takanobu Kato [a], Masayuki Shirakura [b], Daisuke Akazawa [a], Koji Ishii [a], Hideki Aizaki [a], Yumi Kanegae [c], Yoshiharu Matsuura [d], Izumu Saito [c], Takaji Wakita [a], Tetsuro Suzuki [e,**]

[a] *Department of Virology II, National Institute of Infectious Diseases, 1-23-1 Toyama, Shinjuku-ku, Tokyo 162-8640, Japan*
[b] *Influenza Virus Research Center, National Institute of Infectious Diseases, Tokyo 208-0011, Japan*
[c] *Institute of Medical Science, University of Tokyo, Tokyo 108-8639, Japan*
[d] *Research Institute for Microbial Diseases, Osaka University, Osaka 565-0871, Japan*
[e] *Department of Infectious Diseases, Hamamatsu University School of Medicine, 1-20-1 Handayama, Higashi-ku, Hamamatsu, Shizuoka 431-3192, Japan*

ARTICLE INFO

ABSTRACT

In this study, we compared the entry processes of *trans*-complemented hepatitis C virus particles (HCVtcp), cell culture-produced HCV (HCVcc) and HCV pseudoparticles (HCVpp). Anti-CD81 antibody reduced the entry of HCVtcp and HCVcc to almost background levels, and that of HCVpp by approximately 50%. Apolipoprotein E-dependent infection was observed with HCVtcp and HCVcc, but not with HCVpp, suggesting that the HCVtcp system is more relevant as a model of HCV infection than HCVpp. We improved the productivity of HCVtcp by introducing adapted mutations and by deleting sequences not required for replication from the subgenomic replicon construct. Furthermore, blind passage of the HCVtcp in packaging cells resulted in a novel mutation in the NS3 region, N1586D, which contributed to assembly of infectious virus. These results demonstrate that our plasmid-based system for efficient production of HCVtcp is beneficial for studying HCV life cycles, particularly in viral assembly and infection.

Introduction

Over 170 million people worldwide are chronically infected with hepatitis C virus (HCV), and are at risk of developing chronic liver diseases (Hoofnagle, 2002). HCV is an enveloped virus of the family *Flaviviridae*, and its genome is a positive-strand RNA consisting of the 5′-untranslated region (UTR), an open reading frame encoding viral proteins (core, E1, E2, p7, NS2, NS3, NS4A, NS4B, NS5A, and NS5B) and the 3′-UTR (Suzuki et al., 2007).

Host–virus interactions are required during the initial steps of viral infection. It was previously reported that CD81 (Bartosch et al., 2003a, b; McKeating et al., 2004; Pileri et al., 1998), scavenger receptor class B type I (Bartosch et al., 2003a, b; Scarselli et al., 2002), claudin-1 (Evans et al., 2007; Liu et al., 2009) and occludin (Benedicto et al., 2009; Evans et al., 2007; Liu et al., 2009; Ploss et al., 2009) are critical molecules for HCV entry into cells. CD81 interacts with HCV E2 via a second extracellular loop (Bartosch et al., 2003a, b; Hsu et al., 2003) and its role in the internalization process was confirmed (Cormier et al., 2004; Flint et al., 2006). It has also been shown that infectious

* Corresponding author. Fax: +81 3 5285 1161.
** Corresponding author. Fax: +81 53 435 2338.
E-mail addresses: ryosuke@nih.go.jp (R. Suzuki),
tesuzuki@hama-med.ac.jp (T. Suzuki).

HCV particles produced in cell cultures (HCVcc) exist as apolipoprotein E (ApoE)-enriched lipoprotein particles (Chang et al., 2007) and that ApoE is important for HCV infectivity (Owen et al., 2009).

Investigation of HCV had been hampered by difficulties in amplifying the virus in vitro before development of robust cell culture systems based on JFH-1 isolates (Lindenbach et al., 2005; Wakita et al., 2005; Zhong et al., 2005). Retrovirus-based HCV pseudoparticles (HCVpp), in which cell entry is dependent on HCV glycoproteins, have been used to study virus entry (Bartosch et al., 2003a; Hsu et al., 2003). Vesicular stomatis virus (VSV)-based pseudotypic viruses bearing HCV E1 and E2 and replication-competent recombinant VSV encoding HCV envelopes have also been available as surrogate models for studies of HCV infection (Mazumdar et al., 2011; Tani et al., 2007).

It was recently shown that HCV subgenomic replicons can be packaged when structural proteins are supplied in *trans* (Adair et al., 2009; Ishii et al., 2008; Masaki et al., 2010; Steinmann et al., 2008). These *trans*-complemented HCV particles (HCVtcp) are infectious, but support only single-round infection and are unable to spread. Establishment of flexible systems to efficiently produce HCVtcp should contribute to studying HCV assembly, in particular encapsidation of the viral genome, and entry to cells with less stringent biosafety and biosecurity measures. Although single-round infection can be achieved by using the HCVcc system with receptor knock-out

cells, the single-round HCVcc system is not suitable for studying virus entry. We previously described plasmid-based production of HCVcc and HCVtcp (Masaki et al., 2010). Here, we demonstrated that HCVtcp production can be enhanced by introducing the previously reported cell-culture adaptive mutations and by deleting sequences not essential for replication in the subgenomic replicon construct. By providing genotype 1b-derived core-to-p7 in addition to intragenotypic viral proteins, chimeric HCVtcp were generated. Furthermore, blind passage of HCVtcp in the packaging cells resulted in the identification of a novel cell culture-adaptive mutation in NS3 that enables us to establish the efficient production of HCVtcp with structural proteins from various strains. Taken together, our system for producing single-cycle infectious HCV particles should be useful in the study of entry and assembly steps of the HCV life cycles. This technology may also have potential to be the basis for the safer vaccine development.

Results

Enhancement of HCVtcp production by adaptive mutations in E2, p7 and NS2 and by deleting sequences not essential for replication from replicon construct

In our HCVtcp system, the RNA polymerase I (Pol I)-driven replicon plasmid, which carries a dicistronic subgenomic luciferase reporter replicon of JFH-1 strain with a Pol I promoter and terminator (pHH/SGR-Luc), as well as a plasmid containing core-NS2 cDNA under the CAG promoter (pCAGC-NS2) were used (Masaki et al., 2010). In an effort to improve the yield of HCVtcp production, cell culture-adaptive mutations in E2 (N417S), p7 (N765D) and NS2 (Q1012R) which were previously selected from serial passage of HCVcc (Russell et al., 2008) were introduced into the core-NS2 expression plasmid (Fig. 1A) (residues are numbered
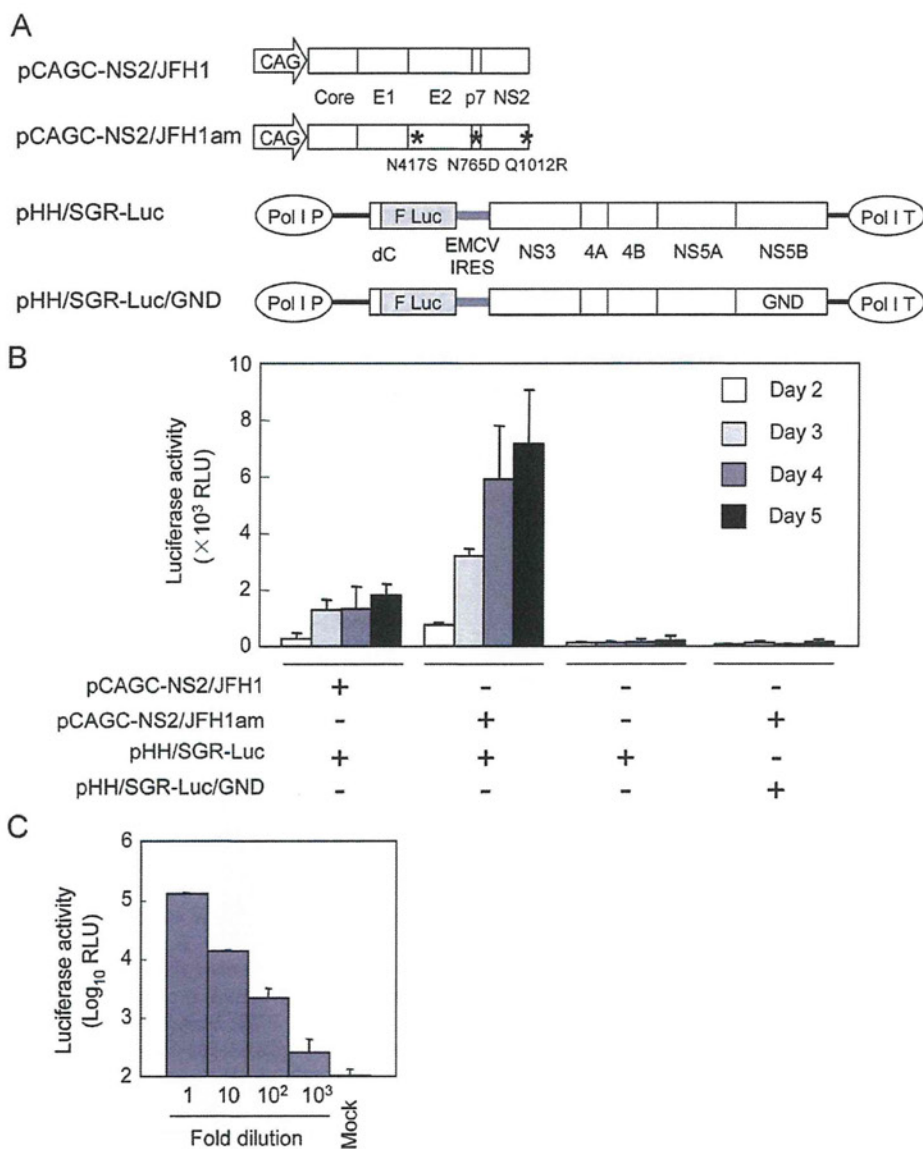
Fig. 1. HCVtcp production by two-plasmid transfection. (A) Schematic representation of plasmids is shown. HCV polyproteins derived from JFH-1 are indicated by white boxes. HCV UTRs are indicated by bold lines. The internal ribosomal entry site from encephalomyocarditis virus (EMCV IRES) is denoted as gray lines. Adaptive mutations are indicated as asterisks. F Luc: firefly luciferase gene; CAG: CAG promoter; Pol I P: RNA polymerase I promoter; Pol I T: RNA polymerase I terminator; GND: replication-deficient GND mutation. (B) Luciferase activity in Huh7.5.1 cells inoculated with supernatant from cells transfected with indicated plasmids at the indicated time points. Data are averages of triplicate values with error bars showing standard deviations. (C) Luciferase activity in cells inoculated with serially diluted HCVtcp.

according to positions within the JFH-1 polyprotein). Supernatants of cells transfected with plasmids (Fig. 1A) were collected and were used to infect Huh7.5.1 cells, which were analyzed by luciferase assay. Introduction of adaptive mutations (pCAGC-NS2/JFH1am) resulted in more than 4-fold higher production of HCVtcp at 5 day post-transfection, as compared to wild-type (WT) (pCAGC-NS2/JFH1) (Fig. 1B), indicating that the adaptive mutations contribute to enhancing HCVtcp production. To confirm that luciferase activity levels in HCVtcp-infected cells are correlated with the number of infectious particles, Huh7.5.1 cells were inoculated with serial dilutions of HCVtcp. Luciferase activity was well correlated with viral load (Fig. 1C), indicating that luciferase assay in HCVtcp-infected cells can be used to quantify HCV infection.

In order to further explore the efficient production of HCVtcp, we generated replicon constructs that lack the luciferase gene or include the partial coding sequences for structural proteins instead of reporter (Fig. 2A). Replication of each replicon in plasmid-transfected cells was then assessed by Western blotting (Fig. 2B). Among the constructs tested, NS5B levels were lowest in cells expressing pHH/SGR-Luc. NS5B levels in cells replicating other replicons appeared to be comparable. Cells were infected with supernatants of cells transfected with each replicon plasmid, along with pCAGC-NS2/JFH1am, followed by infectious unit assay (Fig. 2C). The highest production of HCVtcp was obtained from cells transfected with pHH/SGR, where the luciferase sequence was deleted from pHH/SGR-Luc, thus suggesting that deletion of the sequence not essential for RNA replication in the replicon may contribute to enhancing HCVtcp production.

### Production of chimeric HCVtcp by providing heterologous core-p7

In order to elucidate whether trans-encapsidation of JFH-1 replicon can be achieved by providing core-p7 from other HCV strains, core-NS2 plasmids were constructed (Fig. 3A). In these plasmids, core through the N-terminal 33 aa of NS2, which contains transmembrane domain 1 of NS2, was derived from either H77c (genotype 1a), THpa (genotype 1b), Con1 (genotype 1b) or J6 (genotype 2a) strain. Residual NS2 was derived from JFH-1, as described previously (Pietschmann et al., 2006). HCVtcp was efficiently produced by core-p7 of J6 and THpa strains, but its production was less efficient in the case of Con1 strain. Trans-packaging was not detectable when core-p7 of H77c strain was used (Fig. 3C). Among HCV strains tested, difference in luciferase activity levels in HCVtcp-infected cells (Fig. 3C) were in agreement with that in the viral RNA levels in the culture supernatants of the transfected cells (Fig. 3B). Although the efficacy of trans-complementation was variable among strains, chimeric HCVtcp can be generated by providing genotype 1b-derived core-p7 in addition to intragenotypic viral proteins, and was used in subsequent studies.

ApoE- and CD81-dependent infection by HCVtcp

There is accumulating evidence that apolipoproteins, particularly ApoE, contribute to HCV production and infectivity (Chang et al., 2007; Owen et al., 2009). To determine whether ApoE is involved in infection of target cells by HCVtcp, we infected cells in the presence of increasing concentrations of anti-ApoE antibody.
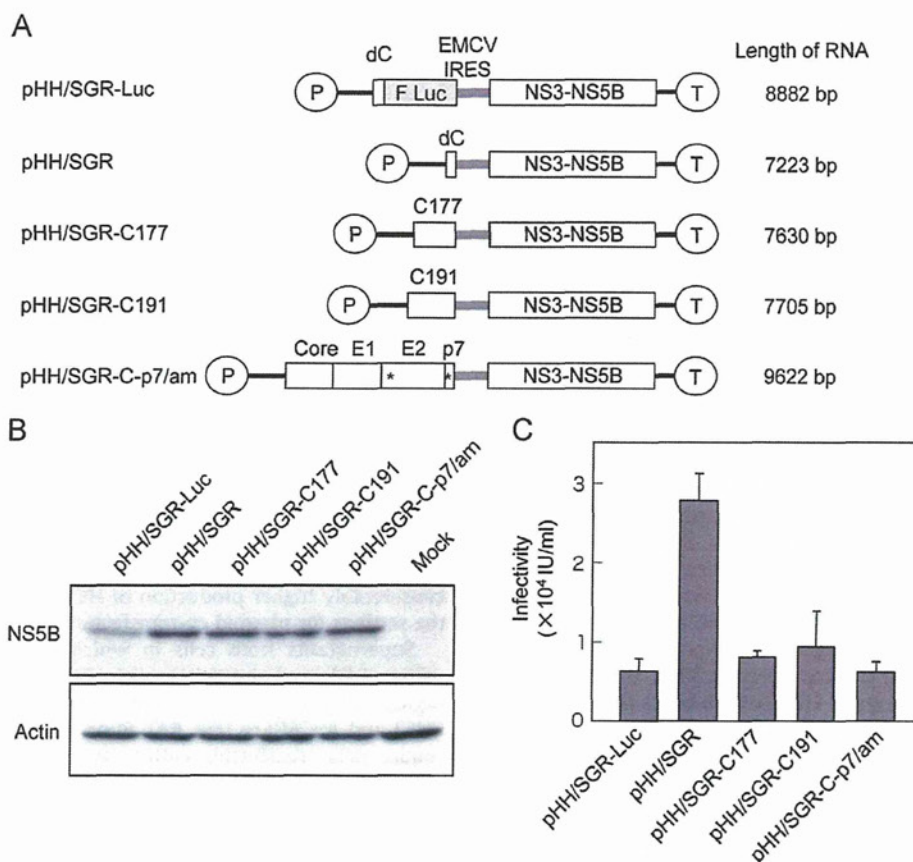
Fig. 2. Production of HCVtcp with different replicon constructs. (A) Schematic representation of plasmids used for production of HCVtcp. Deduced length of transcribed RNA from each construct is shown on the right. HCV polyproteins from JFH-1 strain are indicated by open boxes. HCV UTRs are indicated by bold lines. The EMCV IRES is denoted by gray bars. Adaptive mutations are indicated by asterisks. F Luc: firefly luciferase gene; P: RNA polymerase I promoter; T: RNA polymerase I terminator. (B) Detection of NS5B and actin in Huh7.5.1 cells transfected with indicated plasmids at 4 day post-transfection. (C) Infectivity of culture supernatants from cells transfected with indicated replicon plasmids along with pCAGC-NS2/JFH1am at 4 day post-transfection.
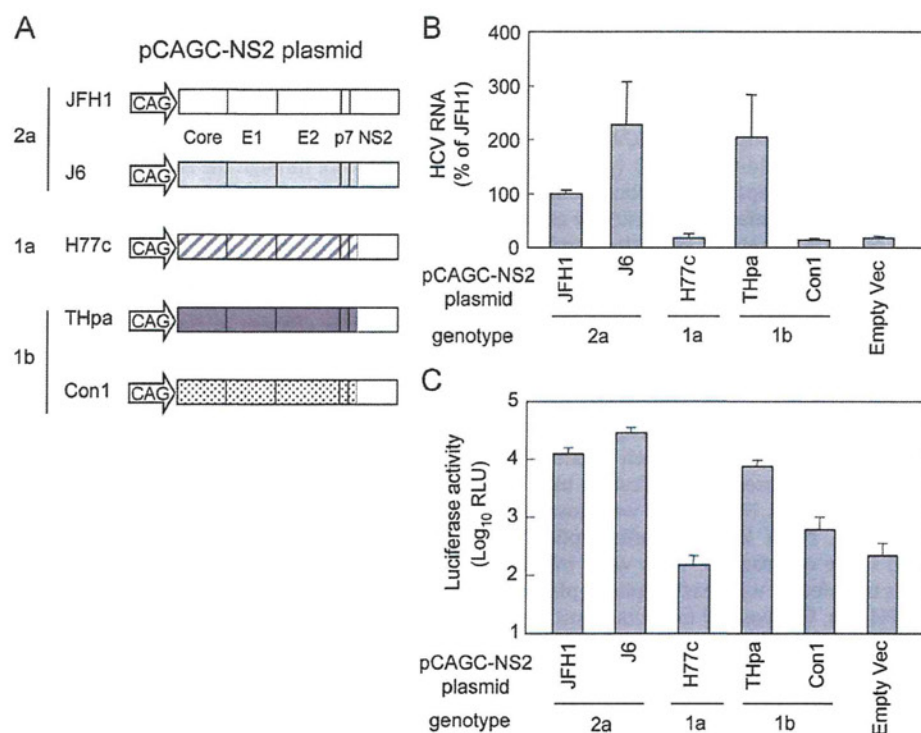
Fig. 3. HCVtcp production with structural proteins from various strains. (A) Schematic representation of plasmids used. HCV polyproteins of JFH-1, J6, H77c, THpa and Con1 strain are shown in the open box, bright gray box, box with diagonal lines, dark gray box and dotted box, respectively. (B) Relative levels of HCV RNA in the supernatant from cells transfected with indicated plasmids along with pHH/SGR-Luc. (C) Luciferase activity in cells inoculated with supernatant from cells transfected with indicated plasmids along with pHH/SGR-Luc at 4 day post-transfection.

pCAGC-NS2/THpa and pCAGC-NS2/JFH1am were used as core-NS2 plasmids for HCVtcp production carrying core-p7 derived from genotypes 1b and 2a (HCVtcp-1b and HCVtcp-2a, respectively). HCVpp derived from JFH-1 and VSVpp were generated and used for comparison. Infection with HCVtcp-1b or HCVtcp-2a was blocked by anti-ApoE antibody in a dose-dependent manner. In contrast, anti-ApoE antibody did not affect infection with HCVpp and VSVpp (Fig. 4A).

The CD81 dependence of infection was also compared between HCVtcp and HCVpp (Fig. 4B). Anti-CD81 antibody inhibited the entry of HCVtcp-1b, HCVtcp-2a, and HCVpp in a dose-dependent manner. The antibody had no effect on VSVpp infection. HCVtcp infection appears to be more sensitive to anti-CD81 antibody when compared with HCVpp infection; more than 60% inhibition was observed at 0.08 μg/mL anti-CD81 antibody for HCVtcp-1b and HCVtcp-2a, whereas approximately 50% inhibition was observed for HCVpp at 2 μg/mL antibody. Neutralization of HCVcc by anti-ApoE and anti-CD81 antibodies was also determined. Antibodies blocked HCVcc infection (Fig. 4C and D), as observed with HCVtcp. These results suggest that ApoE, as well as CD81, play an important role in HCVtcp infection. Thus, HCVtcp may be more useful for evaluating the HCV entry process than HCVpp.

Identification of novel culture-adaptive mutation in NS3 by serial passage of HCVtcp in packaging cells

The HCVtcp system was further applied to analyses of genetic changes during serial passages in target cells. As an initial attempt, supernatants of cells co-transfected with pCAGC-NS2/JFH1am and pHH/SGR were inoculated into Huh7.5.1 cells transiently transfected with pCAGC-NS2/JFH1am. However, infectious titer was lost after repeated inoculation, likely due to low HCVtcp titers and

low efficiency of plasmid transduction (data not shown). To overcome this, we utilized recombinant adenovirus vectors (rAdVs) to provide core-NS2. As we were not able to obtain rAdV directly expressing core-NS2, conditional transgene expression based on a Cre-loxP strategy was employed (Kanegae et al., 1995). We constructed an rAdV containing core-NS2 gene downstream of a stuffer DNA flanked by a pair of loxP sites (AxCALNLH-CNS2). When cells were doubly infected with AxCALNLH-CNS2 and the Cre-expressing rAdV, AxCANCre (Kanegae et al., 1995), the Cre-mediated excisional deletion removed the stuffer DNA, resulting in core-NS2 expression under control of the CAG promoter (Fig. 5A). As expected, tightly regulated production of HCVtcp was observed. The cells infected with AxCANCre and AxCALNLH-CNS2 along with transduction of pHH/SGR-Luc produced HCVtcp at high levels. Production of HCVtcp was undetectable when either AxCANCre or AxCALNLH-CNS2 was not infected (Fig. 5B). The Cre-mediated rAdV expression system appears to have yielded considerably higher production of HCVtcp when compared with the settings for plasmid co-transfection.

Supernatants from cells in which core-NS2 was expressed using rAdVs and the subgenomic RNA derived from pHH/SGR replicated were inoculated into cells infected with AxCALNLH-CNS2 and AxCANCre (Fig. 6A). Blind passage was performed by sequentially transferring culture supernatants to cells infected with the above rAdVs. The two independent 10 blind passages (p10) showed virus titers of $> 1 \times 10^6$ IU/mL, which were markedly higher than those of the passage 0 (p0) stock cultures (4×10^4 IU/mL). Side-by-side infection analysis revealed that the HCVtcp p10 #1 achieved a virus titer approximately 36 times higher than that of HCVtcp p0 on the packaging cells at 6 day post-infection (Fig. 6B). Sequencing of the entire replicon in the supernatants at p10 in two independent experiments revealed
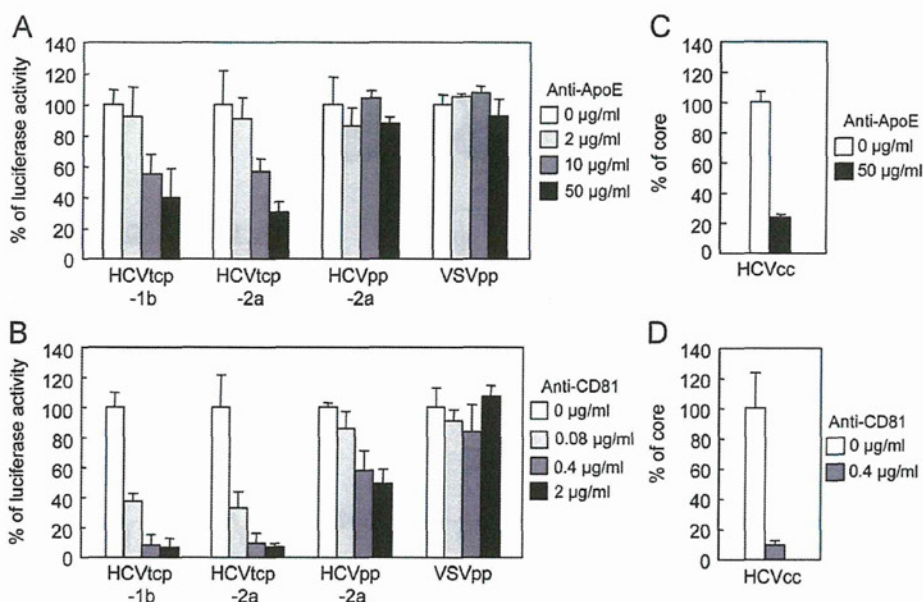
Fig. 4. Effects of anti-ApoE and anti-CD81 antibodies on HCV entry. (A) Aliquots of virus sample were incubated with increasing concentrations of anti-ApoE antibodies for 1 h and were then added to Huh7.5.1 cells. Luciferase activity was determined at 72 h post-infection and is expressed relative to activity without antibodies (white bar). (B) Huh7.5.1 cells were preincubated for 1 h with increasing concentrations of anti-CD81 antibodies, followed by inoculating virus samples. Luciferase activity was determined and expressed as shown in (A). (C) Aliquots of HCVcc were incubated with anti-ApoE antibodies for 1 h and were then added to Huh7.5.1 cells at an MOI of 0.05. Intracellular core levels were quantitated at 24 h post-infection and are expressed relative to levels without antibodies (white bar). (D) Huh7.5.1 cells were preincubated for 1 h with anti-CD81 antibodies. HCVcc infection and measurement of core proteins were performed as indicated in (C).
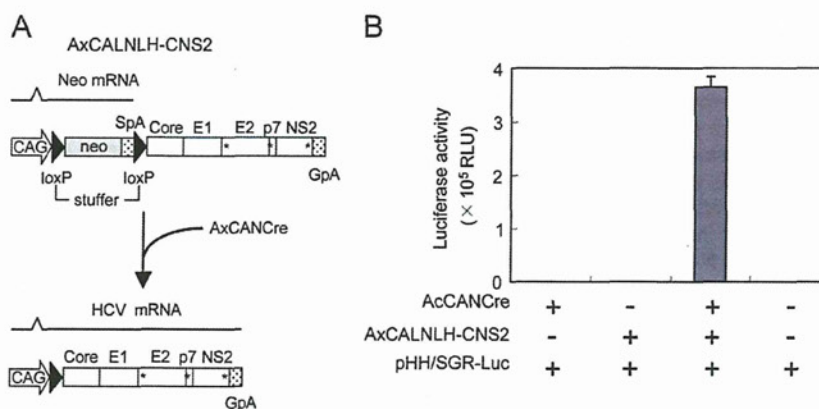

Fig. 5. Transgene activation mediated by rAdVs expressing Cre recombinase under control of CAG promoter. (A) Cre recobminase expressed by AxCANCre recognizes a pair of its target sequences loxP in AxCALNLH-CNS2, and removes the stuffer region resulting in expression of HCV core-NS2 polyprotein by CAG promoter. CAG: CAG promoter; SpA: SV40 early polyA signal; GpA: rabbit b-globin poly(A) signal. (B) Luciferase activity in Huh7.5.1 cells inoculated with 4-day post-transfection culture supernatant from cells transfected with pHH/SGR-Luc, and then infected with indicated rAdVs.

that both passaged HCVtcp had an identical nonsynonymous mutation in the NS3 region (N1586D) (Fig. 6C).

In order to examine the role of NS3 mutation identified on HCV RNA replication and on HCVtcp production, the N1586D mutation was introduced into pHH/SGR-Luc. Luciferase activities of the N1586D-mutated replicon were apparently lower than those of the WT-replicon, thus suggesting that the NS3 mutation reduced viral RNA replication (Fig. 7A). HCV RNA levels in the supernatants of cells transfected with WT- or mutant replicon plasmid along with pCAGC-NS2/JFH1am and luciferase activity in cells inoculated with supernatants from the transfected cells were then determined (Fig. 7B). The viral RNA level secreted from cells replicating the N1586D-mutated replicon was lower than that from cells replicating WT replicon (Fig. 7B, left). By contrast, a significantly higher infectivity of HCVtcp produced from the mutant replicon-cells was observed, as compared to WT replicon-cells (Fig. 7B, right),

suggesting that the adaptive mutation increased the specific infectivity (almost 9-fold) of the virus particles. To further determine whether the N1586D mutation affects infectious viral assembly and/or virus release, we used the CD81-negative Huh-7 subclone, Huh7-25 (Akazawa et al., 2007), which may produce infectious particles, but is not susceptible to HCV entry due to a lack of CD81 expression, therefore allowing us to examine viral assembly and release without the influence of reinfection by produced HCVtcp. Measurement of intracellular and extracellular HCVtcp indicated that Huh7-25 cells replicating the N1586D-mutated replicon produced more infectious virus than WT in both supernatants and cell lysates (Fig. 7C). Thus, it can be concluded that the N1586D mutation contributes to enhanced infectious viral assembly, not RNA replication. We could not exclude the possibility that N1586D mutation affects virus release, since the mutation enhanced extracellular virus titers more than did the intracellular titer.
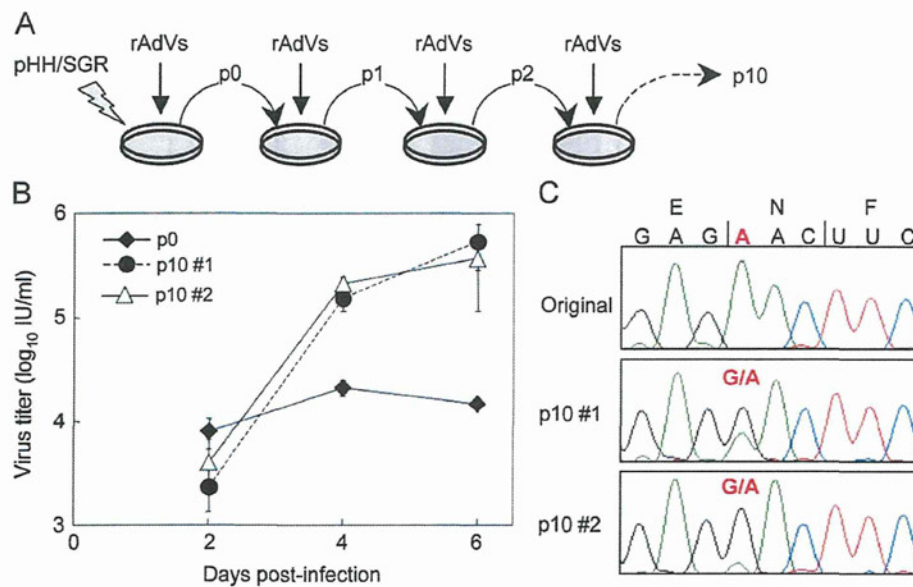
Fig. 6. Genotypic changes in HCVtcp following blind passage. (A) Experimental procedure for blind passage of HCVtcp. Huh7.5.1 cells were transfected with pHH/SGR and were doubly infected with AxCANCre and AxCALNLH-CNS2. Culture fluids were collected and were inoculated into cells infected with AxCANCre and AxCALNLH-CNS2. These procedures were repeated 10 times with two independent samples (#1 and #2). (B) Growth curves of HCVtcp p0 and p10 on Huh7.5.1 cells expressing core-NS2. Cells were infected with HCVtcp at an MOI of 0.05, and medium was collected at the indicated time points and subjected to titration. (C) Nucleotide sequences of original and blind-passaged replicons from HCVtcp. Nucleotides of mutated position are shown in red and bold.

The impact of the N1586D mutation on production of intra- and intergenotypic HCVtcp chimeras was also investigated. The N1586D mutation in the replicon enhanced the production of chimeric HCVtcp by providing core-p7 from all strains examined, although not statistically significant in THpa, and Con1 strains (Fig. 7D). Finally, to determine whether the N1586D mutation was responsible for enhancing HCVcc production, this mutation was introduced into pHHJFH1, which carries the full-length wild-type JFH-1 cDNA (Masaki et al., 2010), yielding pHHJFH1N1586D. The virus titer obtained from cells transfected with the pHHJFH1N1586D was significantly higher than that of WT (Fig. 7E), thus demonstrating that the N1586D mutation enhances yields of HCVcc, in addition to HCVtcp.

Discussion

Single-round infectious viral particles generated by *trans*-packaging systems are considered to be valuable tools for studying virus life cycles, particularly the steps related to entry into target cells, assembly and release of infectious particles. However, limited HCV strains have been applied for the efficient production of HCVtcp to date. In this study, we improved the HCVtcp system in order to enhance the productivity of infectious particles. Production of chimeric HCVtcp by providing genotype 1b-derived core-p7, in addition to intragenotypic viral proteins, was also confirmed. Furthermore, we exploited the system to investigate genetic changes during serial passage of target cells and identified a novel cell culture-adaptive mutation in NS3, which also contributes to enhance the productivity of HCVtcp.

HCVpp (Bartosch et al., 2003a; Hsu et al., 2003) has proven to be a valuable surrogate system by which the study of viral and cellular determinants of the viral entry pathway is possible. Early steps of HCV infection, including the role of HCV glycoprotein heterodimers, receptor binding, internalization and pH-dependent endosomal fusion, have been at least in part mimicked by HCVpp (Lavie et al., 2007). However, as HCVpp is generated in non-hepatic cells such as the human embryo kidney cells 293T, it

is likely that the cell-derived component(s) of HCVpp differ from those of HCVcc. Hepatocytes play a role in maintaining lipid homeostasis in the body by assembling and secreting lipoproteins, including VLDL. It is highly likely that HCV exploits lipid synthesis pathways, as there is a tight link between virion formation and VLDL synthesis. Down-regulation of ApoE considerably reduces HCV production (Benga et al., 2010; Chang et al., 2007; Hishiki et al., 2010; Jiang and Luo, 2009; Owen et al., 2009). Infectivity of HCVcc is also neutralized by anti-ApoE antibodies (Chang et al., 2007). These data suggest that ApoE is important for HCV infectivity. Furthermore, Niemann-Pick C1-like 1 (NPC1L1), involving cholesterol uptake receptor, was recently identified as a host factor for HCV entry (Sainz et al., 2012). Knockdown of NPC1L1 had no effect on the entry of HCVpp whereas HCVcc entry was impaired, possibly due to different cholesterol content of these particles. Here, we found that the anti-ApoE antibody neutralized infection by HCVtcp and HCVcc, but not by HCVpp (Fig. 4A and C), thus suggesting that biogenesis and/or secretion pathways of VLDL are involved in HCVtcp similarly to HCVcc, but not in HCVpp.

We also observed that infectivity of HCVtcp and HCVcc is more efficiently neutralized by the anti-CD81 antibody, as compared to that of HCVpp (Fig. 4B and D). It has recently been reported that E2 of HCVcc contained both high-mannose-type and complex-type glycans, whereas most of the glycans on HCVpp-associated E2 were complex-type, which is matured by Golgi enzymes (Vieyres et al., 2010). Mutational analysis of the N-linked glycosylation sites in E1/E2 demonstrated that several glycans on E2 may affect the sensitivity of HCVpp against antibody neutralization, as well as access of CD81 to its binding site on E2 (Helle et al., 2010). The differences in sensitivity between HCVtcp and HCVpp to neutralization by anti-CD81 antibody observed here may be due to differences in carbohydrate composition of HCV glycoproteins during expression and processing of E1/E2 in cells and morphogenesis of HCVtcp and HCVpp.

By analyzing the various replicons for *trans*-packaging, we observed the highest production of HCVtcp with replicons from pHH/SGR, which lacked sequences not essential for RNA
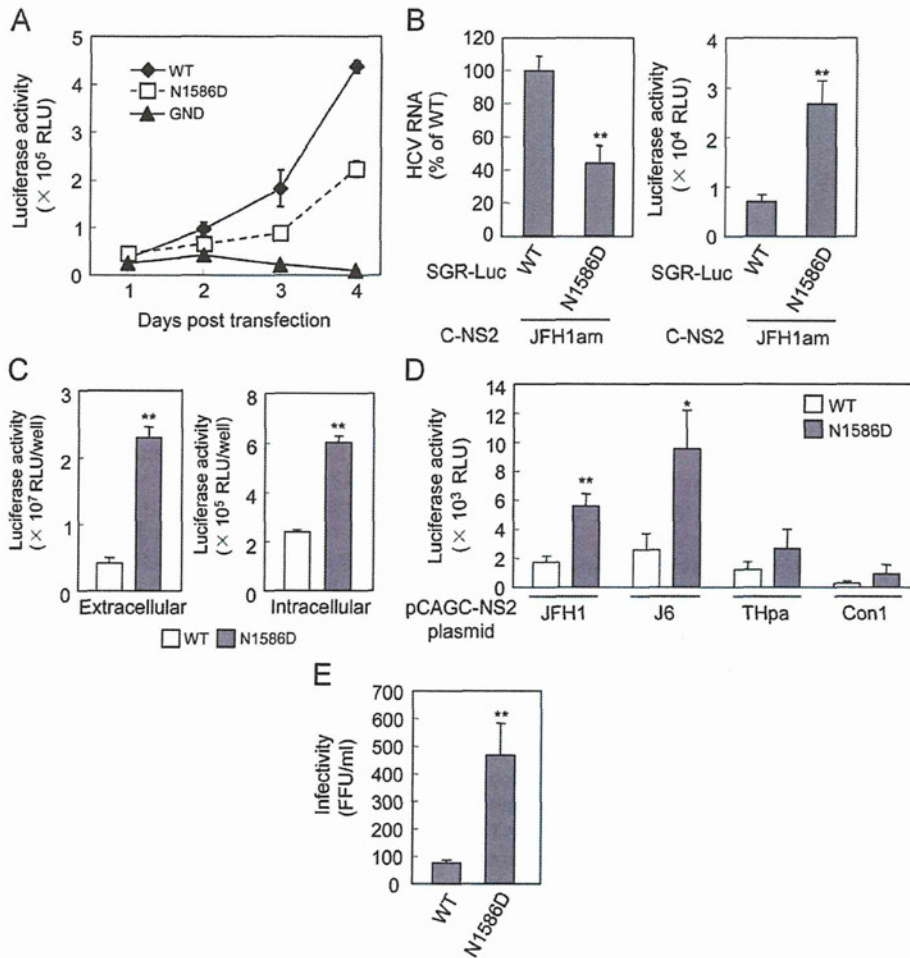
Fig. 7. Effects of N1586D mutation on RNA replication and production of HCVtcp or HCVcc. (A) RNA replication of replicons in cells transfected with pHH/SGR-Luc (WT) or N1586D mutant. Luciferase activities at 1 to 4 day post-transfection were determined. (B) Relative levels of HCV RNA in the supernatants from cells transfected with pHH/SGR-Luc (WT) or N1586D mutant plasmid along with pCAGC-NS2/JFH1am were shown in the left panel. Luciferase activities in cells inoculated with supernatants from cells transfected with indicated plasmids at 4 day post-transfection were shown in the right panel. (C) Luciferase activity in cells inoculated with supernatant and cell lysates from Huh7-25 cells transfected with pHH/SGR-Luc (WT) or N1586D mutant plasmid along with pCAGC-NS2/JFH1am at 5 day post-transfection. (D) Luciferase activity in cells inoculated with culture supernatant from cells transfected with pHH/SGR-Luc (WT) or N1586D mutant plasmid along with indicated core-NS2 plasmids at 4 day post-transfection. (E) Infectivity of supernatant from cells transfected with pHH/JFH1 (WT) or its derivative plasmid containing N1586D mutation at 6 day post-transfection. Statistical differences between WT and N1586D were evaluated using Student's t-test. $^*p < 0.05$, $^{**}p < 0.005$ vs. WT.

replication, while less efficient productivity was observed from pHH/SGR-Luc, pHH/SGR-C177, pHH/SGR-C191 and pHH/SGR-C-p7/am (Fig. 2C). Differences in the replication efficiency of the replicon do not appear to be a major determinant for HCVtcp productivity, at least in the present settings, as all replicon constructs except pHH/SGR-Luc replicated at similar levels, as confirmed by Western blotting (Fig. 2B). Although the shorter viral genome sequence may offer advantages over the longer sequence, further investigation is required in order to understand the molecular mechanisms underlying viral genome packaging. By comparing pHH/SGR vs. pHH/SGR-C177, pHH/SGR-C191 and pHH/SGR-C-p7/am, it is likely that the expression of the structural protein in *cis* does not increase HCVtcp production when sufficient amounts of structural proteins are supplied in *trans*.

Blind passage of HCVtcp in packaging cells infected with rAdVs providing core-NS2 enabled us to identify a novel culture-adaptive mutation in NS3. The N-terminal third of NS3 forms a serine protease, together with NS4A, and its C-terminal two-thirds exhibits RNA helicase and RNA-stimulated NTPase activities. In addition, similarly to flaviviruses (Kummerer and Rice, 2002; Liu et al., 2002), it is now apparent that HCV NS3 is also involved in viral

morphogenesis (Han et al., 2009; Ma et al., 2008), although its precise role and underlying molecular mechanism(s) have not fully been elucidated. Two cell-culture adaptive NS3 mutations which are involved in HCV assembly have been identified. The Q1251L mutation in helicase subdomain 1 resulted in approximately 30-fold higher production of HCV without affecting NS3 enzymatic activities (Ma et al., 2008). The M1290K adaptive mutation was also located in subdomain 1 of the NS3 helicase (Han et al., 2009). The N1586D mutation identified here was located in subdomain 3 of helicase. Analogous to Q1251L and M1290K, the N1586D mutation enhanced the infectious viral assembly by increasing specific infectivity without affecting the efficiency of viral RNA replication. Considering the possibility that NS3 plays a role in linking between the viral replicase and assembly sites (Jones et al., 2011), it is likely that NS3 helicase is one of the determinants for interaction with the structural proteins. Our results, together with earlier studies, suggest that chimeric and defective mutations as well as supplying the viral components in *trans*, function as selective pressures in virion assembly.

In summary, we have established a plasmid-based reverse genetics for efficient production of HCVtcp with structural

proteins from various strains. Single-round infectious HCVtcp can complement the HCVcc and HCVpp systems as a valuable tool for the study of HCV life cycles.

Materials and methods

Cells

Huh7 derivative cell line Huh7.5.1 and Huh7-25 were maintained in Dulbecco modified Eagle medium (DMEM) supplemented with nonessential amino acids, 100 U of penicillin/mL, 100 μg of streptomycin/mL, and 10% fetal bovine serum at 37 °C in a 5% CO_2 incubator.

Plasmids

Plasmids pHHJFH1, pHH/SGR-Luc, pHH/SGR-Luc/GND and pCAG/C-NS2 were as described previously (Masaki et al., 2010). In this study, plasmid pCAG/C-NS2 was designated as pCAGC-NS2/JFH. The plasmid pCAGC-NS2/JFHam having adaptive mutations in E2 (N417S), p7 (N765D), and NS2 (Q1012R) in pCAGC-NS2/JFH was constructed by oligonucleotide-directed mutagenesis. These mutations were also introduced in pHHJFH1, resulting in pHHJFH1am. To generate core-NS2 expression plasmids with different strains of HCV, the cDNA coding core to the first transmembrane region of NS2 (33 amino acids) in pCAGC-NS2/JFH was replaced with the corresponding sequence of the J6 (Lindenbach et al., 2005), H77c (Yanagi et al., 1997), THpa (Shirakura et al., personal communication) and Con1 (Koch and Bartenschlager, 1999) strains. The THpa sequence contained the P to A mutation at 328 aa at E1 in the original TH strain. To generate pHH/SGR, pHH/SGR-Luc was digested with MluI and PmeI, followed by Klenow enzyme treatment and self-ligation to delete the luciferase coding sequence. To generate pHH/SGR-C177, pHH/SGR-C191 and pHH/SGR-C-p7/am, cDNA coding the partial core and luciferase in pHH/SGR-Luc were replaced with coding sequences for mature core (177aa), full-length core (191aa) or core-p7 polyprotein containing adaptive mutations in E2 and p7, respectively. The selected NS3 mutation (N1586D) was introduced into pHH/SGR-Luc and pHHJFH1 by oligonucleotide-directed mutagenesis.

Generation of viruses

HCVcc and HCVtcp were generated as described previously (Masaki et al., 2010). For the production of HCVpp-2a, plasmid pcDNAdeltaC-E1-E2(JFH1)am having adaptive mutations in E2 (N417S) in pcDNAdeltaC-E1-E2(JFH1) (Akazawa et al., 2007) was constructed by oligonucleotide-directed mutagenesis. Murine leukemia virus pseudotypes with VSV G glycoprotein expressing luciferase reporter (VSVpp) were generated in accordance with previously described methods (Akazawa et al., 2007; Bartosch et al., 2003a).

Luciferase assay

Huh7.5.1 cells were seeded onto a 24-well plate at a density of 3×10^4 cells/well 24 h prior to inoculation with reporter viruses. Cells were incubated for 72 h, followed by lysis with 100 μL of lysis buffer. Luciferase activity of the cells was determined using a luciferase assay system (Promega, Madison, WI). All luciferase assays were performed in triplicate.

Quantification of HCV infectivity and HCV RNA

To determine the titers of HCVtcp and HCVcc, Huh7.5.1 cell monolayers prepared in multi-well plates were incubated with dilutions of samples and then replaced with media containing 10% FBS and 0.8% carboxymethyl cellulose. Following incubation for 72 h, monolayers were fixed and immunostained with rabbit polyclonal anti-NS5A antibody, followed by Alexa Fluor 488-conjugated anti-rabbit secondary antibody (Invitrogen), and stained foci or individual cells were counted and used to calculate a titer of focus-forming units (FFU)/mL for spreading infections or infectious units (IU)/mL for non-spreading infections. For intracellular infectivity, the cell pellet was resuspended in culture media, and cells were lysed by four freeze–thaw cycles. Cell debris was pelleted by centrifugation for 5 min at 4000 rpm. Supernatant was collected and used for titration. To determine the amount of HCV RNA in culture supernatants, RNA was extracted from 140 μL of culture medium by QIAamp Viral RNA Mini Kit (QIAGEN, Valencia, CA) and treated with DNase (TURBO DNase; Ambion, Austin, TX) at 37 °C for 1 h. Extracted RNA was further purified by using an RNeasy Mini Kit, which includes RNase-free DNase digestion (QIAGEN). Copy numbers of HCV RNA were determined by real-time quantitative reverse transcription-PCR as described previously (Wakita et al., 2005).

Antibodies

Mouse monoclonal antibodies against actin (AC-15) and CD81 (JS-81) were obtained from Sigma (St. Louis, MO) and BD Biosciences (Franklin Lakes, NJ), respectively. Goat polyclonal antibody to ApoE (LV1479433) was obtained from Millipore (Tokyo, Japan). Anti-NS5A and anti-NS5B antibodies were rabbit polyclonal antibody against synthetic peptides.

Neutralization assay

For neutralization experiments with anti-CD81 antibody, Huh7.5.1 cells were incubated with dilutions of anti-CD81 antibody for 1 h at 37 °C. Cells were then infected with viruses for 5 h at 37 °C. For neutralization experiments with anti-ApoE antibody, viruses were incubated with various concentrations of anti-ApoE antibody at room temperature for 1 h and cells were infected with viruses for 5 h at 37 °C. Following infection, supernatant was removed and cells were incubated with culture medium, and luciferase activity was determined at 3 day post-infection for HCVtcp and pseudotyped viruses. For neutralization experiments with HCVcc generated with pHHJFH1am, a multiplicity of infection (MOI) of 0.05 was used for inoculation, and intracellular core protein levels were monitored by ELISA (Ortho Clinical Diagnostics) at 24 h post-infection.

Immunoblotting

Transfected cells were washed with PBS and incubated with lysis buffer (50 mM Tris–HCl, pH 7.4, 300 mM NaCl, 1% triton X-100). Lysates were then sonicated for 5 min and were added to the same volume of SDS sample buffer. Protein samples were boiled for 10 min, separated by SDS-PAGE, and transferred to PVDF membrane. After blocking, membranes were probed with first antibodies, followed by incubation with peroxidase-conjugated secondary antibody. Antigen–antibody complexes were visualized using an enhanced chemiluminescence detection system (Super Signal West Pico Chemiluminescent Substrate; PIERCE, Rockford, IL), in accordance with the manufacturer's protocols.

Generation of recombinant adenoviruses

rAdV, AxCANCre, expressing Cre recombinase tagged with nuclear localization signal under CAG promoter was prepared as described previously (Baba et al., 2005). The target rAdV AxCALNLH-CNS2 expressing HCV core-NS2 polyprotein with adaptive mutations in E2, p7 and NS2 was generated as follows. Cosmid pAxCALNLwit2 is identical to pAxCALNLw (Sato et al., 1998), except that both the terminal sequences of the rAdV genome are derived from pAxCAwit2 (Fukuda et al., 2006). The core-NS2 fragment obtained from pCAGC-NS2/JFH1am by StuI-EcoRI digestion and subsequent Klenow treatment was inserted into the SwaI site of pAxCALNLwit2. The resultant cosmid pAx-CALNLH-CN2it2 was digested with PacI and transfected into 293 cells to generate rAdV AxCALNLH-CNS2.

Preparation of packaging cells for HCVtcp

Huh7.5.1 cells were coinfected with AxCANCre at an MOI of 1 and AxCALNLH-CNS2 at an MOI of 3 for expression of JFH-1 core-NS2 polyprotein containing the adaptive mutations in E2, p7 and NS2.

RNA preparation, RT-PCR and sequencing

Total cellular RNA was extracted with TRIzol reagent (Invitrogen, Carlsbad, CA), and subjected to reverse transcription with random hexamer and Superscript III reverse transcriptase (Invitrogen). Three fragments of HCV cDNAs that cover the entire HCV subgenomic replicon genome, were amplified by nested PCR with TaKaRa Ex Taq polymerase (Takara, Shiga, Japan). Amplified products were separated by agarose gel electrophoresis, and were used for direct DNA sequencing.

Acknowledgments

References

Adair, R., Patel, A.H., Corless, L., Griffin, S., Rowlands, D.J., McCormick, C.J., 2009. Expression of hepatitis C virus (HCV) structural proteins in trans facilitates encapsidation and transmission of HCV subgenomic RNA. J. Gen. Virol. 90 (Part 4), 833–842.

Akazawa, D., Date, T., Morikawa, K., Murayama, A., Miyamoto, M., Kaga, M., Barth, H., Baumert, T.F., Dubuisson, J., Wakita, T., 2007. CD81 expression is important for the permissiveness of Huh7 cell clones for heterogeneous hepatitis C virus infection. J. Virol. 81 (10), 5036–5045.

Baba, Y., Nakano, M., Yamada, Y., Saito, I., Kanegae, Y., 2005. Practical range of effective dose for Cre recombinase-expressing recombinant adenovirus without cell toxicity in mammalian cells. Microbiol. Immunol. 49 (6), 559–570.

Bartosch, B., Dubuisson, J., Cosset, F.L., 2003a. Infectious hepatitis C virus pseudoparticles containing functional E1-E2 envelope protein complexes. J. Exp. Med. 197 (5), 633–642.

Bartosch, B., Vitelli, A., Granier, C., Goujon, C., Dubuisson, J., Pascale, S., Scarselli, E., Cortese, R., Nicosia, A., Cosset, F.L., 2003b. Cell entry of hepatitis C virus requires a set of co-receptors that include the CD81 tetraspanin and the SR-B1 scavenger receptor. J. Biol. Chem. 278 (43), 41624–41630.

Benedicto, I., Molina-Jimenez, F., Bartosch, B., Cosset, F.L., Lavillette, D., Prieto, J., Moreno-Otero, R., Valenzuela-Fernandez, A., Aldabe, R., Lopez-Cabrera, M., Majano, P.L., 2009. The tight junction-associated protein occludin is required for a postbinding step in hepatitis C virus entry and infection. J. Virol. 83 (16), 8012–8020.

Benga, W.J., Krieger, S.E., Dimitrova, M., Zeisel, M.B., Parnot, M., Lupberger, J., Hildt, E., Luo, G., McLauchlan, J., Baumert, T.F., Schuster, C., 2010. Apolipoprotein E interacts with hepatitis C virus nonstructural protein 5A and determines assembly of infectious particles. Hepatology 51 (1), 43–53.

Chang, K.S., Jiang, J., Cai, Z., Luo, G., 2007. Human apolipoprotein E is required for infectivity and production of hepatitis C virus in cell culture. J. Virol. 81 (24), 13783–13793.

Cormier, E.G., Tsamis, F., Kajumo, F., Durso, R.J., Gardner, J.P., Dragic, T., 2004. CD81 is an entry coreceptor for hepatitis C virus. Proc. Natl. Acad. Sci. USA 101 (19), 7270–7274.

Evans, M.J., von Hahn, T., Tscherne, D.M., Syder, A.J., Panis, M., Wolk, B., Hatziioannou, T., McKeating, J.A., Bieniasz, P.D., Rice, C.M., 2007. Claudin-1 is a hepatitis C virus co-receptor required for a late step in entry. Nature 446 (7137), 801–805.

Flint, M., von Hahn, T., Zhang, J., Farquhar, M., Jones, C.T., Balfe, P., Rice, C.M., McKeating, J.A., 2006. Diverse CD81 proteins support hepatitis C virus infection. J. Virol. 80 (22), 11331–11342.

Fukuda, H., Terashima, M., Koshikawa, M., Kanegae, Y., Saito, I., 2006. Possible mechanism of adenovirus generation from a cloned viral genome tagged with nucleotides at its ends. Microbiol. Immunol. 50 (8), 643–654.

Han, Q., Xu, C., Wu, C., Zhu, W., Yang, R., Chen, X., 2009. Compensatory mutations in NS3 and NS5A proteins enhance the virus production capability of hepatitis C reporter virus. Virus Res. 145 (1), 63–73.

Helle, F., Vieyres, G., Elkrief, L., Popescu, C.I., Wychowski, C., Descamps, V., Castelain, S., Roingeard, P., Duverlie, G., Dubuisson, J., 2010. Role of N-linked glycans in the functions of hepatitis C virus envelope proteins incorporated into infectious virions. J. Virol. 84 (22), 11905–11915.

Hishiki, T., Shimizu, Y., Tobita, R., Sugiyama, K., Ogawa, K., Funami, K., Ohsaki, Y., Fujimoto, T., Takaku, H., Wakita, T., Baumert, T.F., Miyanari, Y., Shimotohno, K., 2010. Infectivity of hepatitis C virus is influenced by association with apolipoprotein E isoforms. J. Virol. 84 (22), 12048–12057.

Hoofnagle, J.H., 2002. Course and outcome of hepatitis C. Hepatology 36 (5 Suppl. 1), S21–9.

Hsu, M., Zhang, J., Flint, M., Logvinoff, C., Cheng-Mayer, C., Rice, C.M., McKeating, J.A., 2003. Hepatitis C virus glycoproteins mediate pH-dependent cell entry of pseudotyped retroviral particles. Proc. Natl. Acad. Sci. USA 100 (12), 7271–7276.

Ishii, K., Murakami, K., Hmwe, S.S., Zhang, B., Li, J., Shirakura, M., Morikawa, K., Suzuki, R., Miyamura, T., Wakita, T., Suzuki, T., 2008. Trans-encapsidation of hepatitis C virus subgenomic replicon RNA with viral structure proteins. Biochem. Biophys. Res. Commun. 371 (3), 446–450.

Jiang, J., Luo, G., 2009. Apolipoprotein E but not B is required for the formation of infectious hepatitis C virus particles. J. Virol. 83 (24), 12680–12691.

Jones, D.M., Atoom, A.M., Zhang, X., Kottilil, S., Russell, R.S., 2011. A genetic interaction between the core and NS3 proteins of hepatitis C virus is essential for production of infectious virus. J. Virol. 85 (23), 12351–12361.

Kanegae, Y., Lee, G., Sato, Y., Tanaka, M., Nakai, M., Sakaki, T., Sugano, S., Saito, I., 1995. Efficient gene activation in mammalian cells by using recombinant adenovirus expressing site-specific Cre recombinase. Nucl. Acids Res. 23 (19), 3816–3821.

Koch, J.O., Bartenschlager, R., 1999. Modulation of hepatitis C virus NS5A hyperphosphorylation by nonstructural proteins NS3, NS4A, and NS4B. J. Virol. 73 (9), 7138–7146.

Kummerer, B.M., Rice, C.M., 2002. Mutations in the yellow fever virus nonstructural protein NS2A selectively block production of infectious particles. J. Virol. 76 (10), 4773–4784.

Lavie, M., Goffard, A., Dubuisson, J., 2007. Assembly of a functional HCV glycoprotein heterodimer. Curr. Issues Mol. Biol. 9 (2), 71–86.

Lindenbach, B.D., Evans, M.J., Syder, A.J., Wolk, B., Tellinghuisen, T.L., Liu, C.C., Maruyama, T., Hynes, R.O., Burton, D.R., McKeating, J.A., Rice, C.M., 2005. Complete replication of hepatitis C virus in cell culture. Science 309 (5734), 623–626.

Liu, S., Yang, W., Shen, L., Turner, J.R., Coyne, C.B., Wang, T., 2009. Tight junction proteins claudin-1 and occludin control hepatitis C virus entry and are downregulated during infection to prevent superinfection. J. Virol. 83 (4), 2011–2014.

Liu, W.J., Sedlak, P.L., Kondratieva, N., Khromykh, A.A., 2002. Complementation analysis of the flavivirus Kunjin NS3 and NS5 proteins defines the minimal regions essential for formation of a replication complex and shows a requirement of NS3 in cis for virus assembly. J. Virol. 76 (21), 10766–10775.

Ma, Y., Yates, J., Liang, Y., Lemon, S.M., Yi, M., 2008. NS3 helicase domains involved in infectious intracellular hepatitis C virus particle assembly. J. Virol. 82 (15), 7624–7639.

Masaki, T., Suzuki, R., Saeed, M., Mori, K., Matsuda, M., Aizaki, H., Ishii, K., Maki, N., Miyamura, T., Matsuura, Y., Wakita, T., Suzuki, T., 2010. Production of infectious hepatitis C virus by using RNA polymerase I-mediated transcription. J. Virol. 84 (11), 5824–5835.

Mazumdar, B., Banerjee, A., Meyer, K., Ray, R., 2011. Hepatitis C virus E1 envelope glycoprotein interacts with apolipoproteins in facilitating entry into hepatocytes. Hepatology 54 (4), 1149–1156.

McKeating, J.A., Zhang, L.Q., Logvinoff, C., Flint, M., Zhang, J., Yu, J., Butera, D., Ho, D.D., Dustin, L.B., Rice, C.M., Balfe, P., 2004. Diverse hepatitis C virus glycoproteins mediate viral infection in a CD81-dependent manner. J. Virol. 78 (16), 8496–8505.

Owen, D.M., Huang, H., Ye, J., Gale Jr., M., 2009. Apolipoprotein E on hepatitis C virion facilitates infection through interaction with low-density lipoprotein receptor. Virology 394 (1), 99–108.

Pietschmann, T., Kaul, A., Koutsoudakis, G., Shavinskaya, A., Kallis, S., Steinmann, E., Abid, K., Negro, F., Dreux, M., Cosset, F.L., Bartenschlager, R., 2006. Construction and characterization of infectious intragenotypic and intergeno- typic hepatitis C virus chimeras. Proc. Natl. Acad. Sci. USA 103 (19), 7408–7413.

Pileri, P., Uematsu, Y., Campagnoli, S., Galli, G., Falugi, F., Petracca, R., Weiner, A.J., Houghton, M., Rosa, D., Grandi, G., Abrignani, S., 1998. Binding of hepatitis C virus to CD81. Science 282 (5390), 938–941.

Ploss, A., Evans, M.J., Gaysinskaya, V.A., Panis, M., You, H., de Jong, Y.P., Rice, C.M., 2009. Human occludin is a hepatitis C virus entry factor required for infection of mouse cells. Nature 457 (7231), 882–886.

Russell, R.S., Meunier, J.C., Takikawa, S., Faulk, K., Engle, R.E., Bukh, J., Purcell, R.H., Emerson, S.U., 2008. Advantages of a single-cycle production assay to study cell culture-adaptive mutations of hepatitis C virus. Proc. Natl. Acad. Sci. USA 105 (11), 4370–4375.

Sainz Jr., B., Barretto, N., Martin, D.N., Hiraga, N., Imamura, M., Hussain, S., Marsh, K.A., Yu, X., Chayama, K., Alrefai, W.A., Uprichard, S.L., 2012. Identification of the Niemann-Pick C1-like 1 cholesterol absorption receptor as a new hepatitis C virus entry factor. Nat. Med. 18 (2), 281–285.

Sato, Y., Tanaka, K., Lee, G., Kanegae, Y., Sakai, Y., Kaneko, S., Nakabayashi, H., Tamaoki, T., Saito, I., 1998. Enhanced and specific gene expression via tissue- specific production of Cre recombinase using adenovirus vector. Biochem. Biophys. Res. Commun. 244 (2), 455–462.

Scarselli, E., Ansuini, H., Cerino, R., Roccasecca, R.M., Acali, S., Filocamo, G., Traboni, C., Nicosia, A., Cortese, R., Vitelli, A., 2002. The human scavenger receptor class B type I is a novel candidate receptor for the hepatitis C virus. EMBO J. 21 (19), 5017–5025.

Steinmann, E., Brohm, C., Kallis, S., Bartenschlager, R., Pietschmann, T., 2008. Efficient trans-encapsidation of hepatitis C virus RNAs into infectious virus- like particles. J. Virol. 82 (14), 7034–7046.

Suzuki, T., Ishii, K., Aizaki, H., Wakita, T., 2007. Hepatitis C viral life cycle. Adv. Drug Deliv. Rev. 59 (12), 1200–1212.

Tani, H., Komoda, Y., Matsuo, E., Suzuki, K., Hamamoto, I., Yamashita, T., Moriishi, K., Fujiyama, K., Kanto, T., Hayashi, N., Owsianka, A., Patel, A.H., Whitt, M.A., Matsuura, Y., 2007. Replication-competent recombinant vesicular stomatitis virus encoding hepatitis C virus envelope proteins. J. Virol. 81 (16), 8601–8612.

Vieyres, G., Thomas, X., Descamps, V., Duverlie, G., Patel, A.H., Dubuisson, J., 2010. Characterization of the envelope glycoproteins associated with infectious hepatitis C virus. J. Virol. 84 (19), 10159–10168.

Wakita, T., Pietschmann, T., Kato, T., Date, T., Miyamoto, M., Zhao, Z., Murthy, K., Habermann, A., Krausslich, H.G., Mizokami, M., Bartenschlager, R., Liang, T.J., 2005. Production of infectious hepatitis C virus in tissue culture from a cloned viral genome. Nat. Med. 11 (7), 791–796.

Yanagi, M., Purcell, R.H., Emerson, S.U., Bukh, J., 1997. Transcripts from a single full-length cDNA clone of hepatitis C virus are infectious when directly transfected into the liver of a chimpanzee. Proc. Natl. Acad. Sci. USA 94 (16), 8738–8743.

Zhong, J., Gastaminza, P., Cheng, G., Kapadia, S., Kato, T., Burton, D.R., Wieland, S.F., Uprichard, S.L., Wakita, T., Chisari, F.V., 2005. Robust hepatitis C virus infection in vitro. Proc. Natl. Acad. Sci. USA 102 (26), 9294–9299.

Visualization and Measurement of ATP Levels in Living Cells Replicating Hepatitis C Virus Genome RNA

Tomomi Ando[1,2], Hiromi Imamura[3], Ryosuke Suzuki[1], Hideki Aizaki[1], Toshiki Watanabe[2], Takaji Wakita[1], Tetsuro Suzuki[4]*

1 Department of Virology II, National Institute of Infectious Diseases, Tokyo, Japan, 2 Graduate School of Frontier Sciences, The University of Tokyo, Tokyo, Japan, 3 The Hakubi Center and Graduate School of Biostudies, Kyoto University, Kyoto, Japan, 4 Hamamatsu University School of Medicine, Department of Infectious Diseases, Hamamatsu, Japan

Abstract

Adenosine 5'-triphosphate (ATP) is the primary energy currency of all living organisms and participates in a variety of cellular processes. Although ATP requirements during viral lifecycles have been examined in a number of studies, a method by which ATP production can be monitored in real-time, and by which ATP can be quantified in individual cells and subcellular compartments, is lacking, thereby hindering studies aimed at elucidating the precise mechanisms by which viral replication energized by ATP is controlled. In this study, we investigated the fluctuation and distribution of ATP in cells during RNA replication of the hepatitis C virus (HCV), a member of the *Flaviviridae* family. We demonstrated that cells involved in viral RNA replication actively consumed ATP, thereby reducing cytoplasmic ATP levels. Subsequently, a method to measure ATP levels at putative subcellular sites of HCV RNA replication in living cells was developed by introducing a recently-established Förster resonance energy transfer (FRET)-based ATP indicator, called ATeam, into the NS5A coding region of the HCV replicon. Using this method, we were able to observe the formation of ATP-enriched dot-like structures, which co-localize with non-structural viral proteins, within the cytoplasm of HCV-replicating cells but not in non-replicating cells. The obtained FRET signals allowed us to estimate ATP concentrations within HCV replicating cells as ~5 mM at possible replicating sites and ~1 mM at peripheral sites that did not appear to be involved in HCV replication. In contrast, cytoplasmic ATP levels in non-replicating Huh-7 cells were estimated as ~2 mM. To our knowledge, this is the first study to demonstrate changes in ATP concentration within cells during replication of the HCV genome and increased ATP levels at distinct sites within replicating cells. ATeam may be a powerful tool for the study of energy metabolism during replication of the viral genome.

Introduction

Adenosine 5'-triphosphate (ATP) is the major energy currency of cells and is involved in a variety of cellular processes, including the virus life cycle, in which ATP-dependent reactions essential for virus multiplication are catalyzed by viral-encoded enzymes or complexes consisting of viral and host-cell proteins [1]. However, the lack of a real-time monitoring system for ATP has hindered studies aimed at elucidating the mechanisms by which cellular processes are controlled through ATP. A method for measuring ATP levels in individual living cells has recently been developed using a genetically-encoded FRET-based indicator for ATP, called ATeam, which employs the epsilon subunit of a bacterial F_0F_1-ATPase [2]. The epsilon subunit has several theoretical advantages for use as an ATP indicator; i) small size (14 kDa), ii) high specific binding to ATP, iii) ATP binding induces a global conformational change and iv) ATP hydrolysis does not occur following binding [3–5]. The affinity of ATeam for ATP can be adjusted by changing various amino acid residues in the ATP-binding domain within the subunit. ATeam has enabled

researchers to examine the subcellular compartment of ATP as well as time-dependent changes in cellular ATP levels under various physiological conditions. For example, the ATeam-based method has been used to demonstrate that ATP levels within the mitochondrial matrix are lower than those in the cytoplasm and the nucleus [2].

Hepatitis C virus (HCV) infects 2–3% of the world population and is a major cause of chronic hepatitis, liver cirrhosis and hepatocellular carcinoma [6–8]. HCV possesses a positive-strand RNA genome and belongs to the family *Flaviviridae*. A precursor polyprotein of ~3000 amino acids is post- or co-translationally processed by both viral and host proteases into at least ten viral products. The nonstructural (NS) proteins NS3, NS4A, NS4B, NS5A and NS5B are necessary and sufficient for autonomous HCV RNA replication. These proteins form a membrane-associated replication complex (RC), in which NS5B is the RNA-dependent RNA polymerase (RdRp) responsible for copying the RNA genome of the virus during replication [9,10]. NS3, in addition to its protease activity, functions as a viral helicase capable of separating duplex RNA and DNA in reactions fuelled

Author Summary

ATP is the major energy currency of living cells. Replication of the virus genome is a physiological mechanism that is known to require energy for operations such as the synthesis of DNA or RNA and their unwinding. However, it has been difficult to comprehend how the ATP level is regulated inside single living cells where the virus replicates, since average ATP values in cell extracts have only been estimated using existing methods for ATP measurement. ATeam, which was established in 2009, is a genetically-encoded Förster resonance energy transfer (FRET)-based indicator for ATP that is composed of a small bacterial protein that specifically binds ATP sandwiched between two fluorescent proteins. In this study, by applying ATeam to the subgenomic replicon system, we have developed a method to monitor ATP at putative subcellular sites of RNA replication of the hepatitis C virus (HCV), a major human pathogen associated with liver disease, in living cells. We show here, for the first time, changes in ATP concentrations at distinct sites within cells undergoing HCV RNA replication. ATeam might open the door to understanding how regulation of ATP can affect the lifecycles of pathogens.

by ATP hydrolysis [11,12]. Consistent with other positive-strand RNA viruses, replication of HCV genomic RNA is believed to occur in membrane-bound vesicles. NS3-NS5B proteins, together with several host-cell proteins, form a membrane-associated RC. The HCV RC is localized to distinct dot-like structures within the cytoplasm of HCV replicating cells and can be detected in detergent-resistant membrane structures [13].

In this study, we first used capillary electrophoresis-time-of-flight mass spectrometry (CE-TOF MS) and the original ATeam method to determine ATP levels in cells infected with HCV or replicating HCV RNA. Using these methods, together with an ATP consumption assay, we demonstrated that ATP is actively consumed in cells in which viral RNA replicates, leading to a reduction in cytoplasmic ATP compared to parental cells. To further understand the fluctuation and distribution of ATP in

HCV replicating cells, we developed a system to monitor ATP at putative subcellular sites of HCV RNA replication in single living cells by applying ATeam technology to the subgenomic replicon system. Our results show that, in viral RNA-replicating cells, ATP levels are elevated at distinct dot-like structures that may play a supportive role in HCV RNA replication, while cytoplasmic levels of ATP decrease.

Results

The concentration of ATP is reduced in HCV-infected cells

As a first approach, the concentration of adenosine nucleotides within HCV-infected and non-infected cells was quantified by CE-TOF MS analysis. ATP levels were approximately 7- and 50-fold higher, respectively, than the levels of ADP and AMP in non-infected Huh-7 cells (Figure 1A). At 9 days post-infection with HCV particles produced from a wild-type JFH-1 isolate [14], the intracellular levels of ATP, ADP and AMP were significantly (52–59%) lower than those in naïve Huh-7 cells (Figure 1A). ATP/ADP and ATP/AMP ratios were comparable among HCV-infected and non-infected cells (Figure 1B). A similar result was obtained using JFH-1/4-5 cells that harbor a HCV subgenomic replicon (SGR) RNA derived from the JFH-1 isolate [15]; the intracellular ATP level of JFH-1/4-5 cells was lower than that of parental Huh-7 cells (Figure S1). These findings are basically consistent with a recent report that phosphorylation-mediated activation of AMP-activated protein kinase is inhibited in cells undergoing HCV genome replication, and that ATP/ADP ratios are similar among cells that do and do not demonstrate HCV replication [16,17].

Measurement of ATP levels in HCV-replicating cells using ATeam

To visualize ATP levels in living cells undergoing HCV genomic replication, one of the ATeam indicators, AT1.03^{YEMK}, which has a high affinity for ATP, was introduced into HCV replicon cells carrying SGR RNA or into parental Huh-7 cells and was imaged using confocal fluorescence microscopy. Consistent with previous observations in HeLa cells [2], this ATP indicator was distributed throughout the cytoplasm. FRET signals (Venus/

A

B
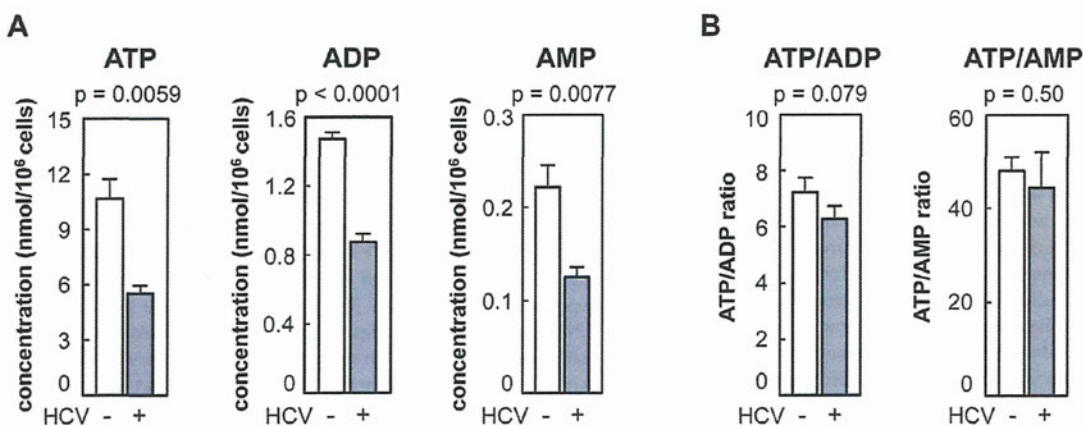
Figure 1. Levels of adenosine nucleotides in HCV-infected and non-infected Huh-7 cells determined by CE-TOF MS. (A) ATP levels were reduced in HCV-infected cells. ATP, ADP, and AMP metabolites in Huh-7 cells with (gray bars) and without (open bars) HCV infection were measured by CE-TOFMS. (B) Ratios of ATP/ADP and ATP/AMP were calculated from the results depicted in (A). All data are presented as means and standard deviation (SD) values for three independent samples. Statistical differences between HCV-infected and non-infected cells were evaluated using Student's t-test.
doi:10.1371/journal.ppat.1002561.g001

CFP fluorescence emission ratios), which reflect ATP levels in living cells, were calculated from the fluorescent images of CFP and Venus, a variant of YFP that is resistant to intracellular pH [18], within the cytoplasm of individual cells. Each independent measurement was plotted as indicated in Figure 2. Uniform Venus/CFP ratios were observed in Huh-7 cells. These ratios were reduced dramatically following combined treatment with 2-deoxyglucose (2DG) and Oligomycin A (OliA), which inhibit glycolysis and the oxidative phosphorylation of ADP to ATP, respectively [2]. When $AT1.03^{YEMK}$ was expressed in the HCV replicon-harboring cells JFH-1/4-1, JFH-1/4-5 (genotype 2a) and NK5.1/0-9 (genotype 1b) [15], Venus/CFP ratios were significantly lower than those seen in parental Huh-7 cells. This result is consistent with the mass spectrometry results shown in Figures 1A and S1. Venus/CFP ratios were more variable in the replicon-carrying cells compared to Huh-7 cells. It is possible that ATP levels in the replicon cells correlate with viral replication levels, which may vary among the cells tested.

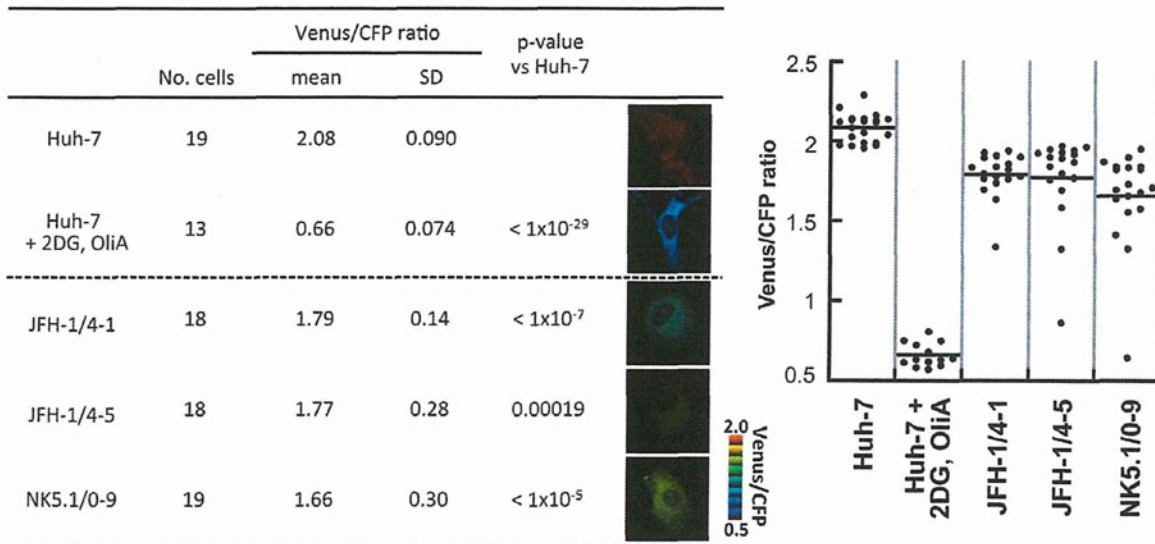## The consumption of ATP is increased in HCV-replicating cells

It has been reported that ATP is involved in different steps in the course of HCV replication such as in the initiation of RNA synthesis by NS5B RdRp [9]. NS3 unwinds RNA in an ATP-dependent manner and may be involved in viral replication [11,19,20]. NS4A has been shown to enhance the ability of the NS3 helicase to bind RNA in the presence of ATP [21]. In addition, ATP is generally used as a material in RNA synthesis. Together with the above results (Figures 1 and 2), one may hypothesize that active consumption of ATP in cells where HCV RNA replicates efficiently results in lower levels of cytoplasmic ATP compared to cells in the absence of the viral RNA. To study the influence of HCV RNA replication on the consumption of ATP in cells, we used permeabilized HCV replicon cells [13,22].

Following the addition of ATP to permeabilized cells, reduced ATP levels were detected using a luciferase-based assay (see Materials and Methods for details). Fifteen minutes after the addition of ATP, ATP levels in permeabilized replicon-carrying cells (JFH-1/4-1, JFH-1/4-5 and NK5.1/0-9) were reduced by 82–95%, and this reduction was greater than that observed in control Huh-7 cells (47%)(Figure 3). When the replication of HCV RNA was inhibited by pre-treatment of the cells with the cytidine analogue inhibitor of HCV NS5B polymerase, PSI-6130 [23,24], for 3 days, the reduction in ATP levels in the replicon cells was comparable to that of Huh-7 cells. A decrease in ATP reduction in the replicon cells was observed even following a 15-min treatment with the inhibitor. An effect of inhibition of viral replication on cytoplasmic ATP levels in replicon cells was also observed by ATeam-based analysis of Venus/CFP ratios following inhibition of replication by IFN-alpha (Figure S2). These results suggest that ATP is actively consumed during viral replication in HCV replicon cells, leading to decreased levels of ATP in the cytoplasm.

Development of a system to monitor ATP levels at putative subcellular sites of HCV replication in single living cells

Moradpour et al. have established functional HCV replicons that have either an epitope tag or the coding sequence for a green fluorescent protein (GFP) inserted in frame close to the C-terminus of NS5A, which they used to demonstrate incorporation of the NS5A-GFP fusion protein into the viral RC [25]. To further investigate intracellular changes in ATP during HCV replication, we generated HCV JFH-1-based subgenomic replicons harboring an ATeam insertion in the 3′ region of NS5A (SGR-ATeam), as

	No. cells	Venus/CFP ratio		p-value vs Huh-7	
		mean	SD		
Huh-7	19	2.08	0.090		
Huh-7 + 2DG, OliA	13	0.66	0.074	$< 1\times10^{-29}$	
JFH-1/4-1	18	1.79	0.14	$< 1\times10^{-7}$	
JFH-1/4-5	18	1.77	0.28	0.00019	
NK5.1/0-9	19	1.66	0.30	$< 1\times10^{-5}$	

Figure 2. ATP fluctuations within the cytoplasm of HCV replicating cells analyzed using the original ATeam. Huh-7 cells carrying a HCV subgenomic replicon, JFH-1/4-1, JFH-1/4-5 (genotype 2a), and NK5.1/0-9 (genotype 1b) and parental Huh-7 cells were transfected with an ATP probe, $AT1.03^{YEMK}$. Forty-eight hours after transfection, the Venus/CFP emission ratio in the cytoplasm of each cell was calculated from fluorescent images acquired with a confocal microscope FV1000 (Olympus). Huh-7 cells treated with 10 mM 2-DG and 10 μg/ml OliA for 20 min were used as a negative control. Data are presented as means and standard deviation values (SD) for each cell. Statistical differences among Huh-7 cells were evaluated using Student's *t*-test. Pseudocolored images of Venus channel/CFP channel ratios of representative cells and a pseudocolor scale are shown. In the graph on the right, each plot indicates the Venus/CFP ratio of each cell. The horizontal lines in the center represent the mean values for each group.
doi:10.1371/journal.ppat.1002561.g002

- 660 -
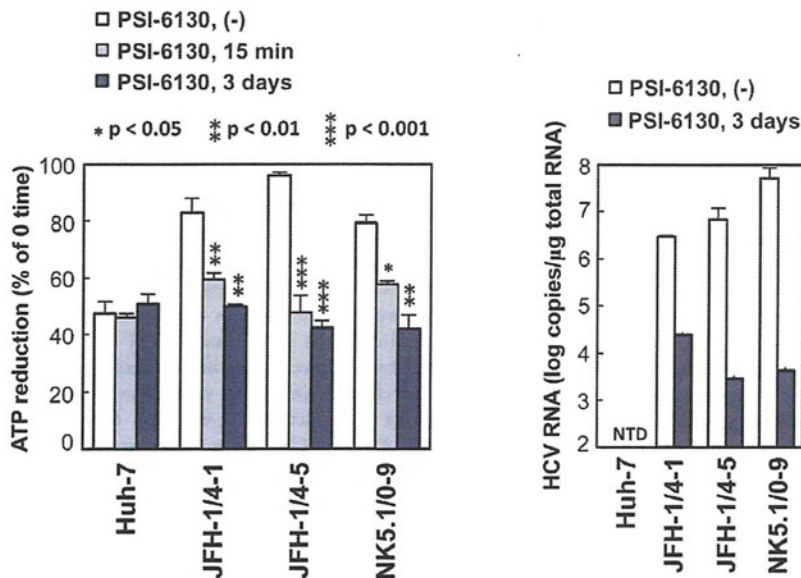
Figure 3. ATP consumption in cells replicating HCV RNA. (Left) The indicated cell lines were pretreated with 10 μM PSI-6130 for 3 days or were cultured in the absence of the drug, followed by trypsinization and permeabilization. ATP-containing reaction buffer plus 10 μM PSI-6130 was added to some of the non-pre-treated cells (PSI-6130, 15 min; light gray bars). ATP-containing PSI-6130-free reaction buffer was added to the rest of the non pre-treated cells (PSI-6130, (−); white bars) and to the pre-treated cells (PSI-6130, 3 days; dark gray bars). After 15 min incubation, ATP levels in cell lysates were measured using a luciferase-based assay. ATP reduction compared to ATP levels at the 0-time point was calculated. The mean values of three independent samples with SD are displayed. Statistical differences between cells treated with and without treatment with PSI-6130 were evaluated using Student's t-test. (Right) HCV RNA titers in cells corresponding to the left panel were determined using real-time quantitative RT-PCR. Data are presented as means and SD for three independent samples. NTD indicates not detected.
doi:10.1371/journal.ppat.1002561.g003

well as plasmids expressing NS5A-ATeam fusion proteins (NS5A-ATeam)(Figures 4A and 4C).

We first tested whether NS5A-ATeam fusion proteins can be used to monitor ATP levels over a range of concentrations in living cells. The Venus/CFP ratios in individual cells expressing NS5A fused either with AT1.03^{YEMK} (Kd = 1.2 mM at 37°C [2]) or with a relatively lower affinity version, AT1.03 (Kd = 3.3 mM at 37°C [2]) were measured. As shown in Figure 4B, differences in the Venus/CFP ratios of NS5A- AT1.03^{YEMK} and NS5A-AT1.03 were similar to those of AT1.03^{YEMK} and AT1.03, although average ratios were lower for NS5A- AT1.03^{YEMK} and NS5A-AT1.03 compared to AT1.03^{YEMK} and AT1.03. In the presence of 2DG and OliA, Venus/CFP ratios of NS5A-AT1.03^{YEMK} were markedly reduced to levels that were comparable to those of AT1.03^{RK}, an inactive mutant with R122K/R126K substitutions [2]. These results demonstrate that NS5A-ATeams can function as ATP indicators, although their dynamic ranges of Venus/CFP ratios are slightly smaller than those of the original, non-fused ATeams.

We next investigated whether the SGR-ATeam could initiate and sustain transient replication of HCV RNA in cells. A RNA polymerase I (Pol I)-derived plasmid, which carries SGR/luc-AT1.03 containing a luciferase reporter gene ([26]; Figure 4C), or its replication-defective mutant were transfected into Huh-7 cells and levels of viral replication were determined by measuring luciferase activity at various time intervals over a five day period (Figure 4D). Although replication of SGR/luc-AT1.03 was delayed compared with parental SGR/luc, the luciferase activity expressed from SGR/luc-AT1.03 rose to approximately a thousand-fold higher than that expressed from SGR/luc-GND-AT1.03 at five days post-transfection. It appears that SGR-

AT1.03, which does not carry the luciferase gene, replicated more efficiently than SGR/luc-AT1.03, as determined by Western blotting of the HCV NS5B protein within cells four days post-transfection (Figure 4E). As indicated in Figure 4F, an abundant protein of the same size as that expected for the NS5A-ATeam fusion protein was observed in cells expressing either NS5A-AT1.03 or SGR-AT1.03, indicating that the NS5A-ATeam fusion protein is stable and is not cleaved during HCV replication. Thus, we concluded that the modified replicon constructs in which the ATeam is incorporated into the NS5A region are functional and remain capable of efficient transient replication of HCV RNA.

Visualization of ATP levels and distinctive features of ATP distribution in cells replicating ATeam-tagged SGR

This SGR-ATeam system that was established to analyze cellular ATP levels was used in living HCV RNA-replicating cells in which membrane-associated RCs are formed through the interaction of viral proteins, including NS5A, and cellular proteins. We compared the subcellular distribution of fluorescent signals expressed from NS5A-ATeams and SGR-ATeams using emission-scanning confocal fluorescence microscopy with a Zeiss META detector. NS5A-AT1.03 and NS5A-AT1.03^{YEMK} were diffusely distributed throughout the cytoplasm (Figure 5A; upper panels). Venus/CFP ratios of NS5A-ATeam constructs were almost constant throughout the cytoplasm (Figure 5A; lower). As expected, Venus/CFP ratios in cells expressing NS5A-AT1.03^{YEMK} were markedly higher than those of NS5A-AT1.03 (Figure 5A; lower). In contrast, cells replicating SGR-AT1.03 and SGR-AT1.03^{YEMK} showed foci of brightly fluorescent dot-like structures in the cytoplasm (Figure 5B; upper panels). Interestingly, some of these fluorescent foci had an apparently higher Venus/

- 661 -